

Zeitschrift: Schweizerische mineralogische und petrographische Mitteilungen = Bulletin suisse de minéralogie et pétrographie

Band: 62 (1982)

Heft: 2

Artikel: The microcline/sanidine transformation isograd in metamorphic regions, I. Composition and structural state of alkali feldspars from granitoid rocks of two N-S traverses across the Aar Massif and Gotthard "Massif", Swiss Alps

Autor: Bambauer, H.U. / Bernotat, W.H.

DOI: <https://doi.org/10.5169/seals-47969>

Nutzungsbedingungen

Die ETH-Bibliothek ist die Anbieterin der digitalisierten Zeitschriften auf E-Periodica. Sie besitzt keine Urheberrechte an den Zeitschriften und ist nicht verantwortlich für deren Inhalte. Die Rechte liegen in der Regel bei den Herausgebern beziehungsweise den externen Rechteinhabern. Das Veröffentlichen von Bildern in Print- und Online-Publikationen sowie auf Social Media-Kanälen oder Webseiten ist nur mit vorheriger Genehmigung der Rechteinhaber erlaubt. [Mehr erfahren](#)

Conditions d'utilisation

L'ETH Library est le fournisseur des revues numérisées. Elle ne détient aucun droit d'auteur sur les revues et n'est pas responsable de leur contenu. En règle générale, les droits sont détenus par les éditeurs ou les détenteurs de droits externes. La reproduction d'images dans des publications imprimées ou en ligne ainsi que sur des canaux de médias sociaux ou des sites web n'est autorisée qu'avec l'accord préalable des détenteurs des droits. [En savoir plus](#)

Terms of use

The ETH Library is the provider of the digitised journals. It does not own any copyrights to the journals and is not responsible for their content. The rights usually lie with the publishers or the external rights holders. Publishing images in print and online publications, as well as on social media channels or websites, is only permitted with the prior consent of the rights holders. [Find out more](#)

Download PDF: 29.04.2026

ETH-Bibliothek Zürich, E-Periodica, <https://www.e-periodica.ch>

The Microcline/Sanidine Transformation Isograd in Metamorphic Regions

I. Composition and structural state of alkali feldspars from granitoid rocks of two N-S traverses across the Aar Massif and Gotthard "Massif", Swiss Alps

by *H. U. Bambauer* and *W. H. Bernotat* *

Abstract

The perthitic alkali feldspars from granitoid rocks of the Aar Massif and Gotthard "Massif" (Central Swiss Alps) were investigated along two N-S traverses (St. Gotthard and Val Medel) by optical and X-ray powder methods. The Na-feldspar of the perthites is always low albite. Two types of microscopically different K-feldspar were observed: 1. Optically "monoclinic" and more or less homogeneous orthoclase displaying variable structural states, ranging from high to low microcline. 2. Low microcline with distinct cross hatching of twins. Along the St. Gotthard traverse, a discontinuous change of structural state was found in the central Aare granite between Wassen and Göschenen: to the north, the K-feldspar is low microcline (1 to 4 mol% Ab, $t_{10}-t_{1m} \sim 1.0$, $2V_x \sim 75-88^\circ$), to the south, structurally variable high microcline (2.5-6.5 mol% Ab, $t_{10}-t_{1m} \sim 0.0-0.4$, $2V_x \sim 53-75^\circ$), is found together with variable amounts of low microcline. This "K-feldspar discontinuity" is interpreted as a relic of the transformation isograd sanidine $T_{diff} \sim 450^\circ\text{C}$ microcline, which is the result of the late Alpine metamorphism.

Zusammenfassung

Die perthitischen Alkalifeldspäte der granitischen Gesteine des Aar-Massivs und des Gotthard-«Massivs» (Zentrale Schweizer Alpen) wurden in zwei Profilen (St. Gotthard und Val Medel) optisch und mit Röntgen-Pulvermethoden untersucht. Der Na-Feldspat in den Perthiten erwies sich stets als Tief-Albit. Mikroskopisch liessen sich zwei Typen von K-Feldspat unterscheiden: 1. Optisch «monokliner», mehr oder weniger homogener Orthoklas, in dem variable strukturelle Zustände gefunden wurden, die von Hoch- bis Tief-Mikroclin reichen. 2. Tief-Mikroclin mit deutlicher Zwillingsgitterung. Im Profil St. Gotthard wurde zwischen Wassen und Göschenen im Zentralen Aaregranit ein diskontinuierlicher Wechsel des strukturellen Zustands gefunden: nach Norden Tief-Mikroclin (1 bis 4 Mol% Ab, $t_{10}-t_{1m} \sim 1.0$, $2V_x \sim 75-88^\circ$), nach Süden strukturell variabler Hoch-Mikroclin (2,5 bis 6,5 Mol% Ab, $t_{10}-t_{1m} \sim 0,0$ bis $0,4$, $2V_x \sim 53-75^\circ$), zusammen mit wechselnden Anteilen Tief-Mikroclin. Diese «K-Feldspat-Diskontinuität» wird als ein Relikt der spätalpidischen Transformationsisograde Sanidin $T_{diff} \sim 450^\circ\text{C}$ Mikroclin interpretiert.

*) Institut für Mineralogie, Universität Münster, Corrensstrasse 24, D-4400 Münster, Fed. Rep. Germany.

Introduction

The Al,Si order/disorder transition in feldspars is the most frequent polymorphism to be observed in the earth's crust. The relation between temperature and Al,Si distribution in K-rich alkali feldspars – so far not fully investigated by experiments – extends over the broad range from low grade metamorphism to sanidinite facies. Meantime, it is sufficiently well known that this transition, because of very sluggish kinetics and thus a strong tendency to disequilibrium, cannot be used as geothermometer over the complete range of metamorphic temperatures.

The number of systematic regional investigations on rock-forming, K-rich alkali feldspars is not very large. Optical data, IR spectra, triclinicity Δ and lattice parameters allow – with a different degree of evidence – conclusions on the structural state of a feldspar. On the basis of such data, more or less extended ranges of “frozen” structural states of K-feldspar were found within single granitic plutons or regional metamorphic rock complexes. But so far, the complete range between low microcline and high sanidine has not yet been reported. GUIDOTTI et al. (1973), COLLERSON (1976) and DORA (1976) reported on examples from metamorphic regions which they identified on the basis of the lattice parameters. These authors show that only limited genetical conclusions can be drawn from their data. The decisive observation was made by STEIGER & HART (1967). They found that the K-feldspars in the contact aureole of the Eldora quartz-monzonite stock (Colorado) showed a *discontinuous* change of structural state over a certain distance from the contact. They explain this discontinuity as inheritance of the transition microcline-“orthoclase”. WRIGHT (1967), in an additional investigation, follows this interpretation and for the first time mentioned the possibility to use this transformation as an isograd in regional metamorphic terrains. On the basis of optical measurements VOLL (1969) found the “K-feldspar discontinuity” in traverses across the contact aureole of the Ballachulish granite in the Scottish Highlands. He also showed that it is likely to be present in the regional metamorphic Dalradian, were the metamorphic zonation was hidden in the critical region by overlaying sediments. Using lattice parameters, KROLL (1980b) found in the Moine Series a systematic change in the ratio of coexisting monoclinic K-feldspar to low microcline, but no K-feldspar discontinuity.

In the regional metamorphic area of the Tauern window (Hohe Tauern, Tyrol), KARL (1959) and RAITH (1971) were the first ones to show a regional distribution of different K-feldspars on the basis of optical data: low microcline in lower-grade greenschist facies rocks, whereas “orthoclase” (KARL) or “monoclinic to weakly triclinic K-feldspar” (RAITH), were found in higher-grade rocks. RAASE & MORTEANI (1976) showed that the transition between these two groups can be traced as an isograd for nearly 60 km. Nearly at the same time first

CENTRAL SWISS ALPS

- +++ stilpnomelane - in
- stilpnomelane - out
- - - staurolite
- An > 85 mol %

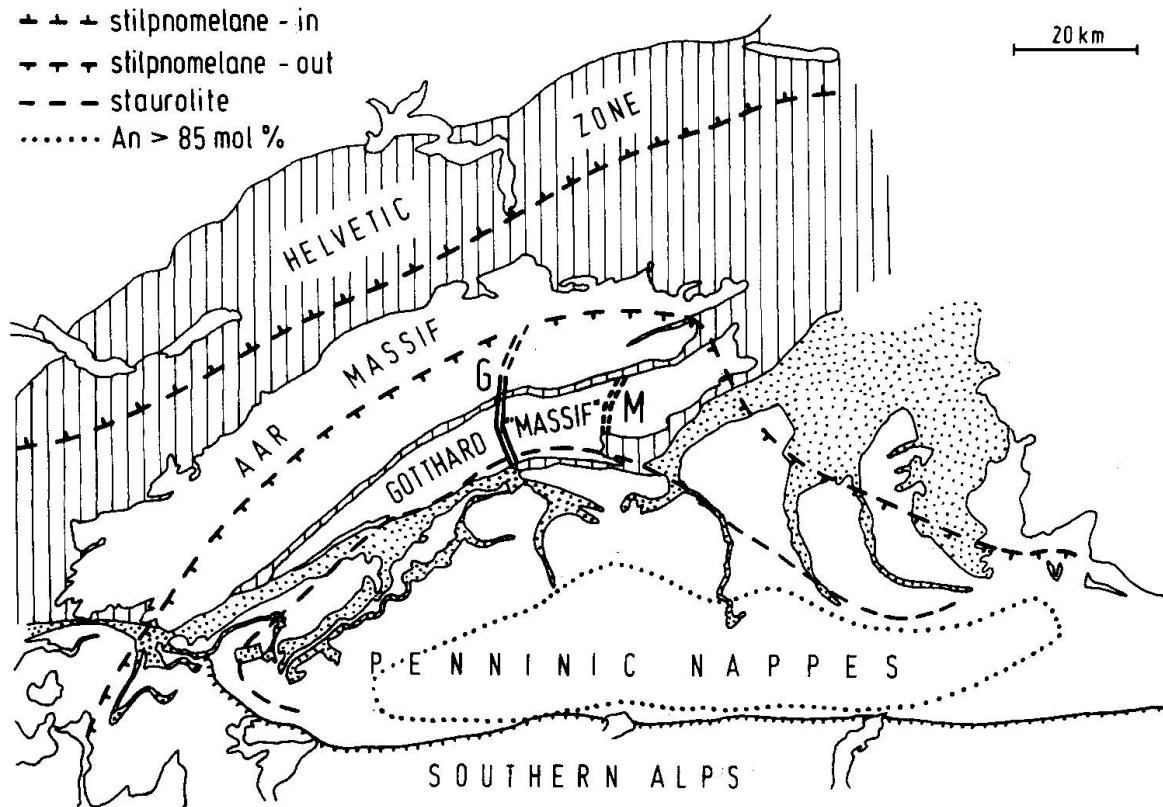


Fig. 1 Sketch map of tectonic units of the Central Swiss Alps. Alpine metamorphic zonation after E. WENK and E. NIGGLI taken from NIGGLI (1974). G = St. Gotthard traverse with Gotthard highway tunnel (solid lines), M = Val Medel traverse.

evidence of the K-feldspar discontinuity in the regional metamorphic area of the Central Swiss Alps was given (BAMBAUER & BERNOTAT 1976). In a next step, BERNOTAT & BAMBAUER (1980) used it as an isograd. They interpreted the discontinuity as an inheritance of the diffusive transformation microcline/sanidine (LAVES 1960). Since it is generally accepted that $T_{diff} < 500^{\circ}\text{C}$, the K-feldspar discontinuity may develop under conditions of higher-grade greenschist facies. One can expect from the review given by FREY et al. (1974) that appropriate conditions were reached in both Alpine regions mentioned. As a result of late Alpine metamorphism (Leontine phase¹) which reached its climax during mid-Tertiary, a marked, concentric metamorphic zonation developed in the Central Swiss Alps, which grades from the central Lepontine¹ area of amphibolite facies over greenschist facies into an outer zone of very low grade metamorphism (Fig. 1). Detailed information for example is given by E. JÄGER, E. NIG-

¹ The geographical term Lepontine Alps and the temporal term Lepontine phase are to be clearly distinguished (compare E. WENK, 1975, p. 121).

GLI & E. WENK (1967), E. WENK & KELLER (1969), E. NIGGLI (1970), EVANS & TROMMSDORFF (1970), JÄGER (1973), FREY (1974), and WAGNER et al. (1977). So far, systematical investigations of the structural state of rock-forming K-feldspars are mostly limited to the central area of highest metamorphic grade: LAVES & VISWANATHAN (1967), H. R. WENK (1967), VISWANATHAN (1968), HISS (1979), HAFNER & LOIDA (1980).

During the late stage of Alpine mineralization, a variety of hydrothermal fissure parageneses formed. They also show, corresponding to the metamorphic zonation, distinct regional trends, indicated by chemistry (WEIBEL, 1961) and structural state (NISSEN, 1967) of adularia, or by the trace element concentration (BAMBAUER et al., 1962) and by fluid inclusions (POTY et al., 1974; FREY et al., 1980) of fissure quartz.

As shown in Fig. 1, the Gotthard highway tunnel cuts the northern metamorphic zonation nearly perpendicular and reaches to the south the outer part of the amphibolite facies. We have chosen this *St. Gotthard traverse* as the main point of our investigation. Thereby, in the course of the tunnel construction, detailed petrographic mapping of the tunnel profile and fresh samples were available. Moreover, the tunnel is part of section 5 of the Swiss Geotraverse Basel-Chiasso (RYBACH, 1976; RYBACH et al., 1980), and thus our special work is connected with the large scale geological, geophysical, and petrological investigations of this research project. In addition, the samples from this traverse were investigated in a cooperation with us by G. Voll (Cologne) who is working on fabric analysis and phase petrology (VOLL, 1976). For comparison, we made additional studies along the *Val Medel traverse*, which is located to the east of the St. Gotthard traverse (Fig. 1). The present, general part I will be followed by the publication of results from regional investigations of the microcline/sanidine isograd in the following areas: Central Swiss Alps (part II, BERNOTAT & BAMBAUER, 1982), Tauern Window, Eastern Alps (part III, BERNOTAT & MORTEANI, 1982), Montagne Noire, French Central Massif (part IV, BERNOTAT, in prep.).

Regional Geology and Petrography

The Gotthard highway tunnel cuts the southern Aar Massif and the Gotthard "Massif"² in full width nearly perpendicular to the Alpine strike. In a strongly simplified characterization, both units are built up by intensively deformed paragneisses (pre-Caledonian sediments) and orthogneisses (pre-Hercynian granites), in which Hercynian granites intruded. These are affected only by the

² The Gotthard Massif is no longer interpreted as autochthonic central massif in the old sense by alpine geologists. In the following we use Gotthard "Massif" or only Gotthard to describe the corresponding tectonic and petrographic unit.

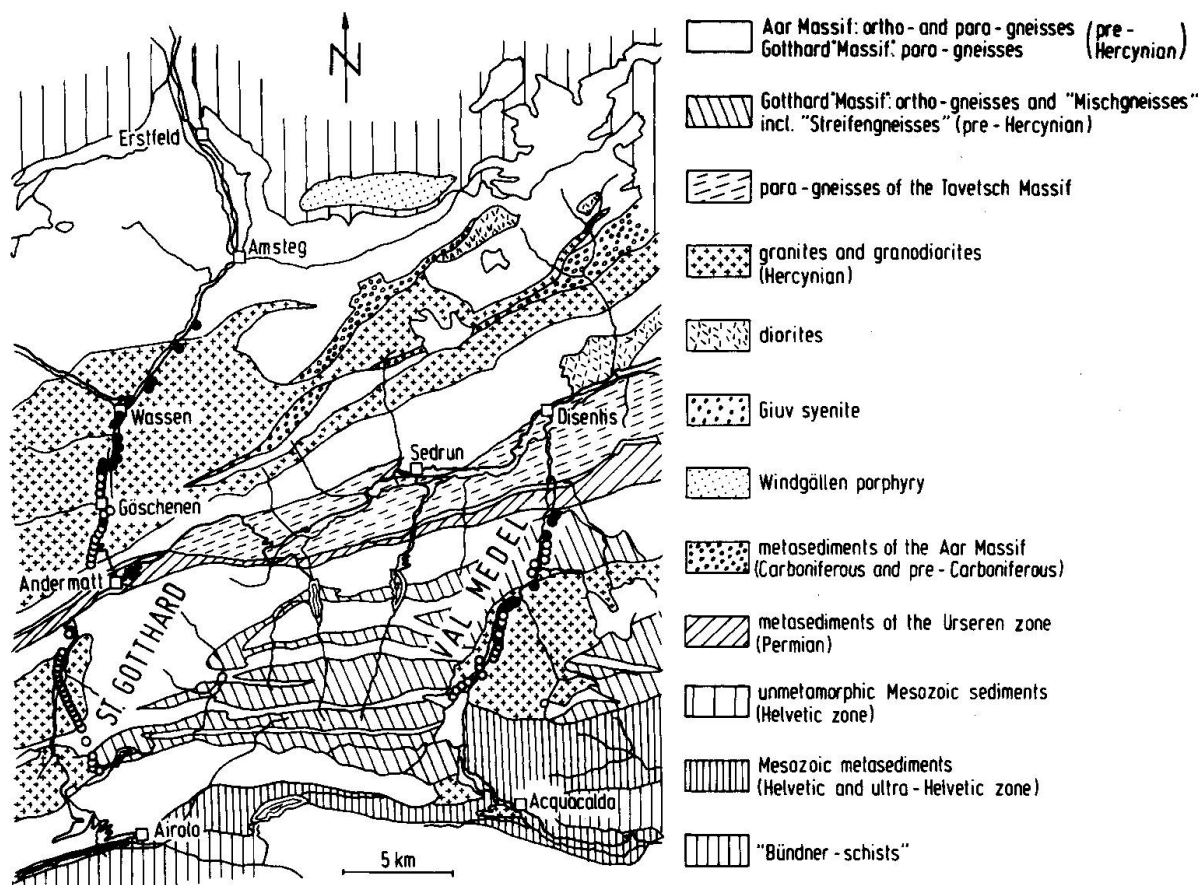


Fig. 2 Geologic map of a section of the Aar Massif and Gotthard "Massif", simplified after LABHART (1977), taken from BAMBAUER (1978). The St. Gotthard traverse (G) and the Val Medel traverse (M) are indicated by the sequences of sample localities: open circles = high microcline (with or without low microcline), filled circles = low microcline (occasionally with minor traces of high microcline).

Alpine deformation which is, in general, much weaker than the Hercynian deformation. The massifs are divided by the Urseren zone, which is composed of Alpine metamorphic, Permo-Carboniferous to Mesozoic sediments. Fig. 2 shows the relevant geological units in some detail. The degree of Alpine deformation and recrystallization increases from the northern Aar Massif - with indications of a rather brittle behaviour - to the southern Gotthard "Massif" and farther to the Penninic nappes - with more plastic behaviour. Some local observations of this kind were made already by AMBÜHL (1930), and, especially for the feldspars, by H. M. HUBER (1943); but a clear understanding of the fabric development along the whole St. Gotthard traverse was provided for the first time by VOLL (1976). Farther to the south, observations on feldspars are given by HISS (1979). In a thorough discussion of all information available, FREY et al. (1980) show that the degree of Lepontine metamorphism increases from the northern border of the Aar Massif (min. 300°C, 2 Kbar) to the southern border of the Gotthard (max. 550°C, 5 Kbar).

Information about the regional petrography of the St. Gotthard traverse and its environments are given by HÜGI (1941, 1956), W. HUBER (1948), SCHINDLER (1972) for the Aar Massif section, and by AMBÜHL (1929), H.M. Huber (1943), HOFMÄNNER (1964), HAFNER (1958) and STEIGER (1961) for the Gotthard "Massif" section. In addition, the excursion guides by BRÜCKNER et al. (1967) and LABHART (1977), both with very comprehensive references, are recommended.

The Val Medel traverse, chosen for comparison, is situated mainly in the Gotthard "Massif", and therefore the most part of the traverse is confined to the rather uniform Medel granite. The regional petrography is given by WINTERHALTER (1930), E. NIGGLI (1944), H.M. HUBER (1943), and ARNOLD (1970), the Alpine metamorphism is treated by FREY (1969).

The new results from the project "Geotraverse Basel-Chiasso" are summarized in Schweiz. Mineral. Petrogr. Mitt. 56/4 (1976) and Eclogae Geol. Helv. 73/2 (1980).

Remarks on the feldspar nomenclature used

The different use of certain feldspar names has been expressively described by SMITH (1974, I, p. 416ff.). Essentially we follow here the nomenclature used by BAMBAUER (1966): With few exceptions, alkali feldspars of granites and granitic gneisses available to us exist as pseudomorphs³, which display an internal texture of mimetic intergrown domains of various secondary feldspars. They are decomposition products, formed from high temperature mixed crystals by polymorphism and exsolution. A practical nomenclature, which should be useful also for the petrographer working with the microscope, has to distinguish names of the *pseudomorphs* in addition to the names of the *feldspar modifications* of which they consist. The names of the modifications which concern this subject are rather uniformly used in literature. Their definition by the lattice parameters is shown in Figures 8 and 9. The pseudomorphs are much more problematic. Their domain size ranges from microscopic to sub-microscopic (electron microscopic) dimensions. In the latter case we observe bulk optics. With decreasing domain size also x-ray methods will fall below the limit of resolution. Therefore, different names were used for such feldspars depending on the method of investigation. The two names used here, microcline perthite and orthoclase perthite, are concisely defined in Table 1. More detailed information is

³ 1. Transition pseudomorphs (paramorphs) without any change of composition, i. e. microcline after sanidine.

2. Exsolution pseudomorphs without change of the bulk composition, i. e. microcline perthite after (K, Na)-sanidine.

Table 1 Nomenclature used for alkali feldspar pseudomorphs.

Name	Characteristics of the K-feldspar component of perthites	K-feldspar modification
	microscopically \pm <u>homogeneous</u> ,	
orthoclase	<u>monoclinic</u> bulk optics	high microcline
perthite	OAP \perp (010), $2V_x \sim 53 - 108^\circ$ +)	to
	monoclinic or triclinic by using x-ray powder methods	low microcline
	microscopically distinct	
	<u>cross hatching</u> after the	
microcline	microcline law	
perthite	<u>triclinic</u> optics, $2V_x \sim 80 - 88^\circ$	low microcline
	triclinic by using x-ray powder methods	
The Na-feldspar component is always low albite or plagioclase on a micro- to crypto-perthitic scale		
+) $2V_x > 90^\circ$: so-called iso-orthoclase (iso-microcline)		

given in the following text. Thus, the name orthoclase, understood in very different ways, is used here to denote the *microscopical appearance* of those K-feldspar pseudomorphs which do not show microscopically visible cross hatching after the microcline law, but have in general monoclinic bulk optics. They may or may not have undulatory extinction. This corresponds to the name orthoclase used by petrographers. It is characterized optically by O.A.P. \perp (010), $2V_x \sim 50-85^\circ$ (compare WINCHELL, 1950). This term covers «common orthoclase» used by LAVES (1960) and orthoclase used by MARFUNIN (1962). The x-ray powder diagram may show variable triclinicity or reach the frequent limiting case "x-ray monoclinic". See also p. 201.

Methods

(a) Sampling

The *St. Gotthard* traverse cuts series of various granites to granitic gneisses, and paragneisses (Fig. 2). It is bordered to the north and south by rocks which

contain only little (Erstfelder Gneiss in the north) or no K-feldspar (Tremola series in the south); the Urseren zone causes a gap within the traverse of about 2 km width. Sampling was done in two sections: In the security tunnel beside the Gotthard highway tunnel in distances of about 25 m (in rare exceptions 100 m), and in fresh outcrops along the line of the highway under construction, in more irregular distances.

The *Val Medel traverse* (Fig. 2), cutting series of ortho- and paragneisses, and the Medel granite body, is bordered to the north by the Urseren zone and to the south by the Scopi anticline, both consisting of K-feldspar-free metasediments. Sampling was done in the rather fresh outcrops along the Lukmanier pass road in more irregular distances. In both traverses, most of the appropriate rocks comprise large (1 to max. 3 cm) phenocrysts or augen of K-feldspar (Table 2 and 3). They are thought to be pre-Alpine. Whenever possible, all investigations were done with these large, fairly well comparable «crystals». Only in the cases they were lacking, K-feldspar fractions were isolated from the rock. However, these samples did not show any significant difference in the local variation of data.

Table 2 Sample localities (topographic coordinates) and optic axial angles $2V_x$ of K-feldspar of perthites from granites and gneisses along the St. Gotthard traverse between Amsteg (N) and Airolo (S).

(a) Phenocrysts from the central Aare granite, Aar Massif. Outcrops between Amsteg (N) and Göschenen (S).

sample No.	coordinates *	$2V_x$ [°]
GPS 68	691800/177350	82, 84, 89, 89
GPS 53	691750/176900	77, 82, 86, 87
GPS 55	691250/176550	81, 83, 86, 87, 87
GPS 56	690050/174900	80, 80, 84, 86, 88
GPS 47	689650/174400	81, 83, 86
GPS 57	689100/173850	82, 84, 86
GPS 61	688400/171150	78, 80, 81, 83, 90
SZA 4567	688625/172250	78, 80, 82, 82, 85, 88
SZA 4568	688600/172000	77, 78, 81, 83, 84, 88
SZA 4569	688500/171700	78, 79, 80, 81, 83, 87
SZA 4570	688200/171200	81, 81, 82, 84, 85, 88
SZA 4571	688275/170575	74, 76, 80, 82, 82, 87
SZA 4572	688275/170050	82, 82, 83, 85, 85
SZA 4573	688300/169800	76, 80, 81, 84, 88
SZA 4574	688250/169600	72, 77, 79, 84, 85, 86
SZA 4575	688125/169350	68, 69, 70, 76, 77, 80, 82
SZA 4576	688200/169050	80, 81, 82, 85, 86

(b) Phenocrysts and augen from the central Aare granite and the southern Aare gneiss, Aar Massif, respectively. Localities from within the Gotthard highway tunnel.

sample No. **	$2V_x [^\circ]$
GSN 240	84, 88
GSN 590	80, 84, 86, 87
GSN 800	80, 81, 82, 86, 87
GSN 920	83, 84, 84, 85, 87
GSN 1159	80, 84, 85, 85, 86
GSN 1220	80, 80, 84, 84, 86, 88
GSN 1230	80, 83
GSN 1380	84, 85, 86, 86, 88
GSN 1840	76, 79
GSN 1890	63, 67, 80, 85, 85, 86, 87, 87, 88, 88
GSN 1980	72, 80, 82, 84, 87, 87, 87, 87, 88, 88
GSN 2010	78, 80, 82, 82, 83, 83, 88, 88, 88, 90
GSN 2400	79, 82, 83
GSN 2460	67, 68, 75, 82, 83, 84, 86, 86, 87, 89
GSN 2480	68, 70, 71, 72, 80, 83, 87, 87
GSN 2605	84, 86, 87
GSN 3150	69, 72, 81, 81, 82, 83, 84, 86, 88
GSN 3180	82, 85, 87, 87, 87
GSN 3390	62, 68, 69, 73
GSN 3745	60, 61, 62
GSN 3902	74, 80, 83

(c) Phenocrysts (augen) from the Gamsboden gneiss, northern Gotthard "Massif". Localities from within the Gotthard highway tunnel.

sample No. **	$2V_x [^\circ]$	sample No. **	$2V_x [^\circ]$
GSN 7202	55, 60, 64, 64	GSS 6501	68, 71, 74, 75, 76
GSN 7450	64, 64, 65, 67, 84	GSS 6401	65, 65, 66
GSN 7840	61, 63, 77	GSS 6304	64, 70, 70
GSS 7803	66, 69, 74	GSS 5998	61, 62, 66, 73
GSS 7311	60, 69, 72, 81	GSS 5790	69, 70, 71, 73, 77, 78
GSS 7004	62, 68, 74	GSS 5580	64, 65

(d) Phenocrysts (augen) from the Fibbia gneiss, southern Gotthard "Massif". Localities from within the Gotthard highway tunnel.

sample No. **	$2V_x [^\circ]$	sample No. **	$2V_x [^\circ]$
GSS 5352	72, 77	GSS 3765	60, 70, 82
GSS 4560	60, 65, 66, 70	GSS 3689	61, 62, 66, 67

* Landeskarten der Schweiz (state maps of Switzerland), Blatt (sheet) 1211 (Meiental), 1212 (Amsteg), 1231 (Urseren).

** The sample number GSN gives the distance (meters) from the northern tunnel entry at Göschenen, GSS the distance from the southern entry at Airolo.

Microscopic inspection of all feldspar specimen investigated, did not reveal much neomineralization of adularia. It has to be considered that adularia with eventually quite different structural states (BAMBAUER & LAVES, 1960) may be found not only in younger fissures, but also as overgrowth of older K-feldspar (VOLL, 1976). Locally, more or less complete chess board albitization may be observed. In the case of regional feldspar investigations, from our experience, we warn of choosing samples for detailed x-ray work without thorough microscopical inspection.

(b) Optical methods

As far as possible, oriented thin sections were prepared of the large K-feldspars. In sections // (001) the perthitic albite and the cross hatching of the microcline twins are best observed, especially in the case of very faint and diffusive cross hatching. Sections $\perp [100]$ were used for the measurement of $2V_x$ by the U-stage. The optic axial angle $2V_x$ was measured on numerous K-feldspars of the same rock sample and occasionally on different parts of the same feldspar. Where possible, measurements were made on the more or less homogeneous orthoclases. If they were not available, cross hatched microclines were measured in addition. All measurements were made conoscopically by using a Zeiss U-stage and the procedure used by BAMBAUER & LAVES (1960) and LAVES & VISWANATHAN (1967). When perfectly adjusted, this U-stage allows a measuring area of $> 60 \mu\text{m}$ in diameter. In many cases microperthitic albite could be screened, but measurement even of well developed single twin domains of microcline was possible only in few exceptions. Therefore, practically all axial angles given are average axial angles of pseudomorphs. According to MARFUNIN (1961) the influence of averaging is small. Where possible, small axial

Table 3 Sample localities (topographic coordinates) and optic axial angles $2V_x$ of K-feldspar of perthites from granites and gneisses along the Val Medel traverse between Val S. Placi (north of Disentis) and Lukmanier pass (south).

(a) K-feldspars of gneisses and gneissic pegmatites from Val S. Placi, Aar Massif.

Aar Massif.		
sample No.	coordinates*	$2V_x$ [°]
SZA 1239	708550/174975	80, 84, 85, 86, 87
SZA 1240	708600/174850	82, 82, 82, 84, 86
SZA 1241	708650/174750	

(b) K-feldspars of schists, gneisses (schistose pegmatites ?) and "Mischgneisses", from Val Medel between Disentis and Curaglia, Tavetsch Massif.

sample No.	coordinates*	$2V_x$ [°]
SZA 1244	708425/172550	
SZA 1229	708175/171750	81, 83, 85
SZA 1222	708250/171550	82, 84
SZA 1223	708400/171300	84
SZA 1224	708400/171025	80, 83, 83, 84, 85
SZA 1225	708250/170700	80, 80, 80, 81, 82, 82, 84, 84, 84, 86

(c) Augen from the northern para- and orthogneisses between Curaglia and Acla, Gotthard "Massif".

sample No.	coordinates*	$2V_x$ [°]
SZA 4566	708350/168400	76, 80, 80, 83, 84, 86, 86
SZA 1528	708200/167900	80, 80, 81, 83, 83, 84, 85
SZA 1526	708150/167500	82, 83, 84, 86, 86, 87
SZA 1527	708200/167150	62, 70, 72, 82
SZA 1525	708000/166550	68, 72, 74, 78
SZA 1523	707850/166400	61, 62, 80, 83, 86
SZA 1524	707750/166150	66, 68, 70, 74

angles near 60° were measured directly as $2V_x$ by using both axes. The accuracy did not exceed $\pm 1^\circ$ in most cases. Axial angles $> 70^\circ$ were measured directly as angle V between one optical axis and the acute bisectrix. In general, the isogyres belonging to small angles did not show the sharpness to be expected from a single crystal in the way observed by BAMBAUER & LAVES (1960) in optically homogeneous domains of adularia. The isogyres belonging to large angles were even less distinct to diffusely broadened so that in some cases measuring became impossible. Therefore, the accuracy was hardly better than $\pm 2-3^\circ$. Com-

Table 3 continued

(d) K-feldspars and wherever present phenocrysts from the Medel granite and the Cristallina granodiorite (C) between Acla and Lukmanier pass, Gotthard "Massif".

sample No.	coordinates*	$2V_x [^\circ]$
SZA 1851	707675/165500	82, 82, 83, 84, 84
SZA 1852	707300/165400	80, 84, 84, 86, 86, 86, 90
SZA 1853	706825/164850	80, 82, 83, 84, 84, 85, 86, 88
SZA 1854	706275/164450	78, 79, 80, 81, 82, 83, 85
SZA 1855	706100/164075	82, 82, 84, 86, 89, 89, 89
SZA 1866	706175/163975	68, 69, 71, 76, 79, 80, 83, 84, 85, 87, 87, 88, 89
SZA 1867	706175/163675	
SZA 1868	706175/163450	82, 85, 86, 86, 88, 89
SZA 1856	706000/163275	63, 65, 68, 74, 78, 82, 82, 84, 85, 86, 87, 88, 89
SZA 1876	705975/163025	59, 61, 61, 63, 66, 85, 87
SZA 1857	705900/162925	76, 82, 82, 85, 88, 88
SZA 1871	705875/162650	54, 58, 58, 58, 60, 62, 65, 68
SZA 1858	705825/162575	72, 78, 82
SZA 1869	705725/162300	64, 65, 66, 67, 67, 88, 88, 90
SZA 1859(C)	705675/162225	57, 58, 61, 62, 63, 63, 63
SZA 1865	705200/161925	63, 65, 66, 67, 68, 69, 69, 71, 76
SZA 1860(C)	705150/161250	
SZA 1864(C)	705150/161650	
SZA 1875	705000/161650	61, 64, 66
SZA 1873	704900/161250	53, 59, 60, 65, 68, 68, 70, 71, 72
SZA 1863	704825/161075	59, 62, 62, 63, 65, 65, 68, 69, 69, 72, 87, 89
SZA 1872	704625/160775	55, 57, 67, 73, 83
SZA 1870	704350/160650	58, 58, 60, 66, 67, 67, 69, 72, 76
SZA 1861	704150/160500	56, 59, 60, 62, 62, 63, 68, 70, 73, 73, 73, 74, 76
SZA 1862	704075/160200	55, 59, 60, 60, 62, 63, 66, 67

* Landeskarten der Schweiz (state maps of Switzerland) Blatt (sheet) 1213 (Trun), 1232 (Oberalppass) and 1233 (Greina).

pared to the orthoscopic method, the conosopic method allows a better resolution of the local scatter of $2V$ within a feldspar, a better adjustment of the optical axes, and, by far, faster working. All axial angles measured are given in Tables 2 and 3.

(c) Determination of lattice parameters by x-ray powder methods

In thin section, a part of a large K-feldspar appearing to be suitable for a powder diagram was marked, and then, from the counterpart remaining in the rock slab, a core was taken of about 8 mm³ by using an ultrasonics drilling instrument. The powder diagrams were taken by using an AEG-Guinier-Jagodzinski camera with CuK_{α1}-radiation and a quartz monochromator. As an internal standard pure silicon with $a = 5.43309 \text{ \AA}$ was used; because of too many coincidences, quartz proved to be unsuitable. The exact line positions were read by a high-precision ruler with an accuracy of $\pm 0.01 \text{ mm}$, corresponding to 0.005° of 2θ . By using a computer program for film correction (JAGOKOR, KROLL, 1968), the positions of the powder lines were corrected for the first three lines of Si. Lattice parameters were refined only from those K-feldspars which showed at least 20 lines to be identified unambiguously. The refinement was made by the least square method using the LCLSQ-program of BURNHAM (1962). Lattice parameters and cell volumes are given in Tables 4 and 5. The small core sample used was sufficiently large to allow investigation both of the K- and Na-feldspar of a perthite. But it often was too large to sufficiently allow the resolution of optically visible structural inhomogeneities of the K-feldspar. LAVES & VISWANATHAN (1967) took volumes of about 1.5 mm³ and extremely long exposure times for their small scale correlations of powder data and $2V_x$. BAMBAUER & LAVES (1960), using precession photographs, even took only about 0.01 mm³. HAFNER & LOIDA (1980) found, also using precession photographs, that "crystal fragments of 0.1–0.3 mm size have usually homogeneous, well defined lattices". It remains an open question, whether this is always the case. In case of doubt we should take into consideration chemical and structural inhomogeneities ranging into electron microscopical dimensions (i. e., see BLASCHKE et al., 1974). We consider the sample quantity used here as a reasonable compromise between effort and result.

(d) Calculation of chemical composition from cell volume

The composition of the K-feldspar component of perthites may be calculated from cell volume [\AA^3] by the following empirical formula of STEWART & WRIGHT (1974):

$$\text{Or (mol\%)} = (0.2962 - \sqrt{0.95313 - 0.0013 V}) / 0.18062$$

The compositions calculated are given as Ab-content in Tab. 4 and 5. Although the cell volume is also slightly influenced by the degree of Al, Si order, the resulting changes may be neglected for nearly pure K-feldspar. Control measurements by using our aged microprobe mostly gave too high Ab-values and low accuracy because of insufficient resolution.

Table 4 Lattice parameters, chemical composition and Al,Si distribution of perthites from granites and gneisses along the St. Gotthard traverse. For sample localities see Table 2. Though the refinement of lattice parameters resulted in calculated errors of 0.001 Å or 0.01° (often less), it is more realistic to assume errors of ± 0.002 Å and $\pm 0.02^\circ$.

sample No.	a [Å]	b [Å]	c [Å]	α [°]	β [°]	γ [°]	volume [Å ³]	Ab [mol%]	Al occupancy	lines
									t_1 t_2	$2t_1$ $2t_2$ No.
GPS 53A	8.5841	12.9675	7.2254	90.640	115.960	87.620	722.49	1.3	1.00 0.00	0.00 0.00 45
GPS 56/3(1)	8.5772	12.9696	7.2236	90.630	115.934	87.729	722.07	2.5	0.97 0.01	0.02 0.02 36
SZA 4568	8.5773	12.9663	7.2231	90.647	115.956	87.663	721.67	3.7	0.99 0.00	0.02 0.02 40
SZA 4570	8.5821	12.9630	7.2234	90.659	115.950	87.660	721.96	2.9	1.00 0.00	0.00 0.00 37
SZA 4573	8.5829	12.9671	7.2218	90.694	115.979	87.693	721.94	2.9	0.98 0.00	0.02 0.02 36
SZA 4575	8.5829	12.9851	7.2042	90.000	115.999	90.000	721.65	3.8	0.39 0.39	0.22 0.22 27
GSN 240 S	8.5802	12.9646	7.2225	90.650	115.950	87.650	721.79	3.4	0.99 0.00	0.01 0.01 46
GSN 240(2)	8.5819	12.9676	7.2252	90.651	115.945	87.665	722.41	1.5	0.99 0.00	0.00 0.00 27
GSN 800 S	8.5778	12.9624	7.2238	90.666	115.956	87.648	721.56	4.0	1.00 0.00	0.00 0.00 38
GSN 1220	8.5764	12.9631	7.2237	90.668	115.951	87.638	721.50	4.2	1.00 0.00	0.00 0.00 38
GSN 1980 S	8.5806	12.9646	7.2232	90.650	115.950	87.630	721.88	3.1	1.00 0.00	0.00 0.00 52
GSN 1980	8.5790	12.9665	7.2244	90.655	115.956	87.634	721.94	2.9	1.00 0.00	0.00 0.00 54
GSN 1990 S	8.5797	12.9648	7.2246	90.640	115.950	87.640	721.96	2.9	1.00 0.00	0.00 0.00 43
GSN 3150 S	8.5812	12.9646	7.2232	90.650	115.930	87.660	722.07	2.5	1.00 0.00	0.00 0.00 36
GSN 3150	8.5811	12.9651	7.2235	90.665	115.934	87.647	722.09	2.5	1.00 0.00	0.00 0.00
GSN 3500	8.5841	12.9829	7.2071	90.000	116.008	90.000	721.87	3.1	0.40 0.40	0.21 0.21 26
GSN 3720	8.5832	12.9778	7.2086	90.042	116.022	89.891	721.57	4.0	0.43 0.38	0.19 0.19 27
GSN 3745	8.5748	12.9835	7.2058	90.000	116.015	90.000	720.95	5.8	0.39 0.39	0.22 0.22 31
GSN 6355	8.5805	12.9777	7.2096	90.119	116.012	89.497	721.47	4.3	0.52 0.31	0.17 0.17 24
GSN 7200	8.5857	12.9701	7.2139	90.177	116.019	89.487	721.87	3.1	0.54 0.33	0.13 0.13
GSN 7202	8.5845	12.9820	7.2089	89.995	116.042	89.913	721.82	3.3	0.42 0.38	0.20 0.20 29
GSN 7450	8.5811	12.9680	7.2134	90.160	116.000	89.286	721.41	4.5	0.59 0.29	0.12 0.12 24

sample No.	a [Å]	b [Å]	c [Å]	α [°]	β [°]	Y [°]	volume [Å ³]	Ab [mol%]	Al occupancy		lines No.	
									t ₁₀	t _{1m} 2t ₂		
GSN 7820	8.5815	12.9785	7.2086	90.037	116.017	89.937	721.50	4.2	0.42	0.39	0.19	27
GSN 7840/1	8.5786	12.9751	7.2105	90.157	115.999	89.536	721.34	4.7	0.52	0.32	0.16	20
GSN 7840/3	8.5812	12.9701	7.2137	90.237	116.009	89.205	721.50	4.2	0.61	0.27	0.12	18
GSN 7840/4	8.5803	12.9756	7.2135	90.194	116.000	89.282	721.77	3.4	0.58	0.28	0.14	25
GSN 7804/5	8.5796	12.9786	7.2083	90.150	116.006	89.449	721.35	4.7	0.53	0.30	0.18	34
GSN 7840/6	8.5823	12.9779	7.2119	89.987	116.028	89.981	721.80	3.4	0.41	0.41	0.18	32
GSN 7859	8.5810	12.9723	7.2116	90.228	116.012	89.206	721.37	4.6	0.60	0.26	0.14	24
GSN 7917	8.5842	12.9764	7.2104	90.000	116.015	90.000	721.80	3.3	0.41	0.41	0.18	23
GSN 7930	8.5836	12.9789	7.2107	90.055	116.032	89.789	721.81	3.3	0.45	0.36	0.18	23
GSN 7940	8.5789	12.9728	7.2113	90.221	115.997	89.210	721.29	4.8	0.60	0.26	0.14	29
GSN 7950	8.5827	12.9770	7.2117	90.000	116.022	90.000	721.80	3.4	0.41	0.41	0.18	23
GSN 7960	8.5804	12.9770	7.2090	90.084	115.974	89.714	721.62	3.9	0.48	0.36	0.17	37
GSN 8000	8.5809	12.9809	7.2083	90.000	116.015	90.000	721.56	4.0	0.40	0.40	0.20	29
GSN 8007	8.5783	12.9780	7.2097	90.034	115.976	89.911	721.56	4.0	0.43	0.39	0.17	21
GSS 8200	8.5831	12.9794	7.2079	90.051	115.987	89.850	721.80	3.4	0.44	0.38	0.18	26
GSS 8100	8.5808	12.9759	7.2101	90.186	116.008	89.320	721.45	4.4	0.57	0.28	0.16	35
GSS 7995	8.5829	12.9790	7.2095	90.050	116.026	89.789	721.67	3.7	0.45	0.36	0.19	44
GSS 7902	8.5837	12.9784	7.2098	90.085	116.028	89.665	721.72	3.6	0.48	0.34	0.18	32
GSS 7698	8.5832	12.9740	7.2138	90.202	115.990	89.334	722.03	2.7	0.58	0.29	0.13	28
GSS 7498	8.5828	12.9775	7.2103	90.029	116.035	89.826	721.61	3.9	0.45	0.37	0.18	30
GSS 7312	8.5850	12.9717	7.2117	90.000	116.050	90.000	721.52	4.2	0.42	0.42	0.17	27
GSS 7004	8.5844	12.9807	7.2105	90.000	116.033	90.000	721.96	2.9	0.40	0.40	0.19	29
GSS 6800	8.5822	12.9755	7.2130	90.070	116.023	89.804	721.79	3.4	0.46	0.38	0.16	27
GSS 6700	8.5855	12.9803	7.2096	90.030	116.019	89.852	722.02	2.7	0.44	0.38	0.19	30
GSS 6401	8.5796	12.9710	7.2112	90.295	115.974	89.045	721.34	4.7	0.64	0.24	0.12	28

Table 4 continued

sample No.	a [Å]	b [Å]	c [Å]	α [°]	β [°]	γ [°]	volume [Å ³]	Ab [mol%]	Al occupancy t_{10} t_{1m} $2t_2$	lines No.
GSS 6192	8.5792	12.9756	7.2093	90.135	116.016	89.539	721.20	5.1	0.51 0.32 0.17	40
GSS 5998	8.5800	12.9775	7.2105	89.997	116.029	89.890	721.43	4.4	0.43 0.39 0.18	28
GSS 5898	8.5816	12.9772	7.2126	90.115	116.011	89.627	721.86	3.2	0.50 0.34 0.16	24
GSS 5790/2	8.5792	12.9824	7.2060	90.000	116.009	90.000	721.31	4.8	0.39 0.39 0.21	31
GSS 5748	8.5791	12.9754	7.2109	90.000	116.033	90.000	721.26	4.9	0.41 0.41 0.18	27
GSS 5728/2	8.5815	12.9816	7.2118	90.103	116.026	89.641	721.92	3.0	0.49 0.34 0.18	34
GSS 5700	8.5822	12.9734	7.2099	90.116	116.006	89.050	721.46	4.3	0.49 0.35 0.16	24
GSS 5625	8.5805	12.9708	7.2110	90.244	115.984	89.187	721.36	4.6	0.61 0.26 0.13	20
GSS 5580	8.5782	12.9703	7.2110	90.175	116.017	89.388	720.96	5.8	0.56 0.30 0.14	33
GSS 5550	8.5788	12.9720	7.2098	90.027	116.005	89.392	721.10	5.4	0.44 0.39 0.17	22
GSS 5540	8.5843	12.9781	7.2112	90.036	116.054	89.902	721.74	3.5	0.43 0.39 0.19	22
GSS 5517	8.5785	12.9718	7.2099	90.154	116.005	89.411	721.04	5.6	0.55 0.30 0.15	33
GSS 5468	8.5781	12.9773	7.2127	90.246	115.900	89.153	721.64	3.8	0.61 0.25 0.14	32
GSS 5448	8.5798	12.9768	7.2136	90.237	116.011	89.220	721.73	3.5	0.60 0.26 0.14	38
GSS 5427	8.5807	12.9786	7.2120	90.209	116.006	89.257	721.78	3.4	0.58 0.27 0.15	34
GSS 4150	8.5788	12.9762	7.2106	90.178	115.986	89.347	721.49	4.3	0.56 0.29 0.15	26
GSS 4108	8.5807	12.9804	7.2116	90.045	116.015	89.832	721.85	3.2	0.45 0.38 0.18	29
GSS 3840	8.5822	12.9801	7.2101	90.043	116.027	89.912	721.74	3.5	0.42 0.39 0.19	30
GSS 3765	8.5880	12.9739	7.2112	90.154	116.019	89.622	722.02	2.7	0.50 0.34 0.15	23
GSS 3600	8.5791	12.9799	7.2095	90.139	116.009	89.480	721.48	4.3	0.52 0.30 0.18	32
GSS 3100	8.5855	12.9810	7.2092	90.013	116.021	89.889	722.01	2.7	0.43 0.38 0.19	41

(e) Calculation of Al,Si distributions from lattice parameters

For the routine determination of Al,Si distributions of alkali feldspar from lattice parameters the following methods are available: the bc, $\alpha^*\gamma^*$ method of STEWART & RIBBE (1969), its modifications as b^*c^* , $\alpha^*\gamma^*$ method by SMITH (1974, I), the Tr[110], Tr[1 $\bar{1}$ 0] method of KROLL (1973), and the simple (204)/(060) method of WRIGHT (1968). The Al,Si distributions are given as Al site occupancies t_{1o} , t_{1m} , t_{2o} , t_{2m} (notation after KROLL, 1973) of the four non-equivalent tetrahedral sites T_{1o} , T_{1m} , T_{2o} , T_{2m} (notation after MEGAW, 1956).

When using each of these methods, one has to take into account that the lattice parameters of K-feldspar (at constant temperature and pressure) are a function of at least four essential factors which are: (1) the Na/K ratio, (2) the Al,Si distribution, (3) the lattice distortion between triclinic, sub-microscopical domains which in general are mimetically twinned after the microcline law, (4) the lattice distortion between coherent K-rich and Na-rich domains in cryptoperthite. The third case has been well known a long time ago (GOLDSMITH & LAVES, 1954; HAFNER & LAVES, 1957), but has not been quantitatively investigated. The influence of decreasing domain size and increasing lattice distortion obviously leads to a diminishing of the angles α^* and γ^* as measured, to apparent monoclinic metric (SMITH, 1974, I, p. 267). Also, an influence of unbalanced twinning on the lattice angles is to be expected, and in addition, x-ray monoclinic and triclinic areas may exist side by side within the pseudomorph. These influences are frequently realized in orthoclase (GOLDSMITH & LAVES, 1954; HAFNER & LAVES, 1957). Therefore, the distinction between triclinic microcline and x-ray monoclinic orthoclase, rather commonly used in literature, seems not to be very reasonable, because a difference in Al,Si distribution may or may not exist. As a result of this, we do not use the name orthoclase (definition see p. 191) in the narrow meaning of "x-ray monoclinic non-sanidine", as used by STECK & BURRI (1971), KROLL (1980b), and others. The fourth case also leads to anomalous (strained) lattice parameters, first observed by LAVES (1952). The amount of strain in cryptoperthite may be estimated by the methods of STEWART & WRIGHT (1974) or BERNOTAT (in prep.).

At present, the most reliable measure for Al,Si distributions of alkali feldspar is provided by mean $\langle T-O \rangle$ distances which were determined by structure refinement (RIBBE, 1975). In Table 6 the methods of calculation mentioned above are compared to the $\langle T-O \rangle$ method. The two high microclines Spencer U (BAILEY, 1969) and K 235 (RIBBE & GIBBS, 1975), chosen as examples, show that all methods in question give similar results. Checking the data in closer detail, differences become discernible. It can be seen that the values calculated using the bc, $\alpha^*\gamma^*$ method show the largest deviations. Also, this can be seen from a diagram (not shown here) corresponding to Fig. 10: the $(2t_1-2t_2)$ values, calculated from "bc", show a considerably increased scatter, and compared to the

Table 5 Lattice parameters, chemical composition and Al,Si distribution of perthites from granites and gneisses along the Val Medel traverse. For sample localities see Table 3. Though the refinement of lattice parameters resulted in calculated errors of 0.001 Å or 0.01° (often less), it is more realistic to assume errors of ± 0.002 Å and $\pm 0.02^\circ$.

(a) Augen from the northern para- and orthogneisses.

sample No.	a [Å]	b [Å]	c [Å]	α [°]	β [°]	γ [°]	volume [Å ³]	Ab [mol%]	Al occupancy t_{10} t_{1m} $2t_2$	lines No.
SZA 1527	8.5735	12.9651	7.2211	90.639	115.933	87.720	721.26	4.9	0.98 0.01 0.02	58
SZA 4566	8.5752	12.9639	7.2218	90.646	115.931	87.657	721.38	4.6	0.99 0.00 0.01	61

(b) K-feldspars and wherever present phenocrysts from the Medel granite and the Crystallina granodiorite (C).

sample No.	a [Å]	b [Å]	c [Å]	α [°]	β [°]	γ [°]	volume [Å ³]	Ab [mol%]	Al occupancy t_{10} t_{1m} $2t_2$	lines No.
SAZ 1851	8.5774	12.9644	7.2245	90.647	115.945	87.662	721.78	3.4	1.00 0.00 0.00	31
SAZ 1852	8.5755	12.9655	7.2222	90.693	115.930	87.703	721.57	4.0	0.98 0.01 0.01	49
SAZ 1853/1	8.5773	12.9664	7.2223	90.648	115.933	87.659	721.74	3.5	0.99 0.00 0.01	47
SAZ 1853/2	8.5790	12.9651	7.2215	90.659	115.933	87.641	721.72	3.6	0.99 0.00 0.01	46
SAZ 1854	8.5778	12.9655	7.2229	90.654	115.940	87.681	721.76	3.5	0.99 0.00 0.01	57
SAZ 1855/1	8.5729	12.9657	7.2214	90.652	115.937	87.669	721.22	5.0	0.99 0.00 0.02	40
SAZ 1855(1)	8.5801	12.9641	7.2206	90.650	115.955	87.640	721.53	4.1	0.99 0.00 0.01	30
SAZ 1867	8.5797	12.9625	7.2217	90.673	115.942	87.643	721.60	3.9	1.00 0.00 0.01	45
SAZ 1868	8.5743	12.9646	7.2226	90.646	115.934	87.647	721.40	4.5	1.00 0.00 0.01	68
SAZ 1856	8.5768	12.9755	7.2089	90.202	115.998	89.270	721.02	5.6	0.58 0.27 0.16	31
SAZ 1871(1)	8.5808	12.9607	7.2227	90.659	115.958	87.639	721.59	4.0	1.00 0.00 0.00	28
SAZ 1871(2)	8.5804	12.9819	7.2085	90.000	116.016	90.000	721.59	4.0	0.40 0.40 0.20	25
SAZ 1858	8.5753	12.9625	7.2229	90.623	115.917	87.709	721.53	4.1	0.99 0.01 0.00	36
SAZ 1869	8.5806	12.9814	7.2086	90.094	115.994	89.636	721.71	3.6	0.49 0.33 0.18	39
SAZ 1859(C)	8.5774	12.9657	7.2225	90.675	115.943	87.668	721.67	3.7	0.99 0.00 0.01	32
SAZ 1865	8.5826	12.9781	7.2089	90.046	116.045	89.962	721.42	4.5	0.41 0.39 0.20	39
SAZ 1860(C)	8.5803	12.9780	7.2077	90.000	116.030	90.000	721.20	5.1	0.40 0.40 0.20	25
SAZ 1864(C)	8.5847	12.9790	7.2109	90.040	116.060	89.882	721.76	3.5	0.42 0.38 0.19	28
SAZ 1863	8.5838	12.9773	7.2100	90.054	116.019	89.805	721.75	3.5	0.45 0.37 0.18	32
SAZ 1870	8.5814	12.9794	7.2071	90.032	116.034	89.950	721.29	4.8	0.41 0.39 0.21	45
SAZ 1861/1	8.5765	12.9733	7.2091	90.000	116.030	90.000	720.76	6.4	0.41 0.41 0.18	30
SAZ 1861/2	8.5834	12.9713	7.2103	90.000	116.030	90.000	721.35	4.7	0.42 0.42 0.17	28
SAZ 1862	8.5815	12.9833	7.2081	90.073	116.035	89.694	721.59	3.9	0.46 0.33 0.20	38

reference point K 235 are evidently larger. The two other methods listed in Tab. 6 under (b) appear to be of rather equal quality. In addition, they seem to be less sensitive against strain in cryptoperthite (compare K 235). Indeed, because of the high Or content of the K-feldspars studied here, neither the Na/K ratio nor strain is expected to be of great influence. This has been proven by HAFNER & LOIDA (1980) using single crystal methods. For the sake of a uniform presentation of data we use here the b^*c^* diagram (Fig. 8) and the $\alpha^*\gamma^*$ diagram (Fig. 9). The $(\bar{2}04)/(060)$ method listed in Table 6 under (c) has been proven to be a rapid method, but is less useful in the case of strongly strained cryptoperthite.

Table 6 Comparison of five methods to determine the Al,Si distribution in K-feldspar.

method	Spencer U [*])			K 235 ^{**})		
	t_{10}	t_{1m}	$t_{20}+t_{2m}$	t_{10}	t_{1m}	$t_{20}+t_{2m}$
(a) structure refinement: mean bond length $\ll T-0 \gg$ ¹⁾	0.64	0.24	0.11	0.48	0.32	0.19
(b) lattice parameter refinement						
Tr[110], Tr[1 $\bar{1}$ 0] ²⁾	0.61	0.29	0.10	0.50	0.33	0.16
$\Delta(b^*,c^*)$, $\Delta(\alpha^*,\gamma^*)$ ³⁾	0.63	0.29	0.08	0.50	0.33	0.18
$\Delta(b,c)$, $\Delta(\alpha^*,\gamma^*)$	0.64	0.31	0.05	0.52	0.35	0.13
(c) measurement of 2θ	$t_{10}+t_{1m}$			$t_{10}+t_{1m}$		
$2\theta(060)$, $2\theta(\bar{2}04)$ ⁵⁾	0.94			0.82		

¹ RIBBE (1975)

² KROLL (1980)

³ SMITH (1974)

⁴ STEWART & RIBBE (1969)

⁵ WRIGHT (1968)

* "Microcline", BAILEY (1969)

** "Cryptoperthite", RIBBE & GIBBS (1975)

Since [110] and [1 $\bar{1}$ 0] are the directions with maximal difference in Al,Si order, we use Kroll's method for the calculation of site occupancies. These two translations are calculated from lattice parameters as follows:

$$\text{Tr}[110] = (a^2 + b^2 + 2ab \cos \gamma)^{1/2}$$

$$\text{Tr}[1\bar{1}0] = (a^2 + b^2 - 2ab \cos \gamma)^{1/2}$$

According to KROLL (pers. comm.), the Al occupancies of triclinic K-rich alkali feldspars are calculated, taking the chemical composition into account, by the following equations:

$$t_{1o} = 47.3666 - 6.18192 \cdot \text{Tr}[110] - 24.49293 \cdot \text{Tr}[1\bar{1}0] + 0.79755 N_{\text{Or}}$$

$$t_{1m} = 47.3666 - 23.18872 \cdot \text{Tr}[110] - 7.48612 \cdot \text{Tr}[1\bar{1}0] + 0.79755 N_{\text{Or}}$$

N_{Or} is the molar fraction KAlSi_3O_8 ; the equations are valid for $N_{\text{Or}} = 0.7 - 1.0$ (i.e. for Or > 70 mol%), and for translations given in [Å].

Since $t_{1o} + t_{2o} + t_{1m} + t_{2m} = 1$, and t_{2o} practically equals t_{2m} , it follows:

$$t_2 = t_{2o} = t_{2m} = (1 - t_{1o} - t_{1m})/2.$$

Equations corresponding to the monoclinic case are given by KROLL (1980a). All Al,Si distributions calculated are given in Tab. 4 and 5.

(f) Infra-red spectroscopy

From many alkali feldspar samples an IR spectrum was taken in the range of 400–1000 cm^{-1} , using a grating infra-red spectral photometer Perkin Elmer model 457. As usual, the samples were imbedded into KBr tablets (4 mg of sample into 1 g KBr). In alkali feldspar the increase of Al,Si order is indicated by a particular increase of absorption at approx. 650 cm^{-1} and 540 cm^{-1} . Because of superposition problems, the "degree" of order of a K-feldspar can be recognized only if the amount of Na-feldspar is minor. The absence of the typical absorption of low albite between 700 and 800 cm^{-1} is taken as a criterion for a minor content of Na-feldspar. Thus, following the method of HAFNER & LAVES (1957), samples with predominantly low microcline could be clearly distinguished from those with prevailing high microcline. This method is very useful for rapid routine work with a large number of samples. However, it is unsuitable for fine differentiations, especially if the perthite contains high amounts of albite, high and low microcline together.

Results

(a) Microscopical appearance of alkali feldspars

In general, two large groups of microscopically different alkali feldspars were observed in the rocks along the traverses St. Gotthard and Val Medel:

(1) Microcline perthite: the K-feldspar is distinctly cross hatched, with relatively large, well developed twin domains. The Na-feldspar is vein perthite for the most part (Fig. 3).

(2) Orthoclase perthite: the K-feldspar generally appears turbid with innumerable minute inclusions. Its extinction generally is nearly uniform to irregu-

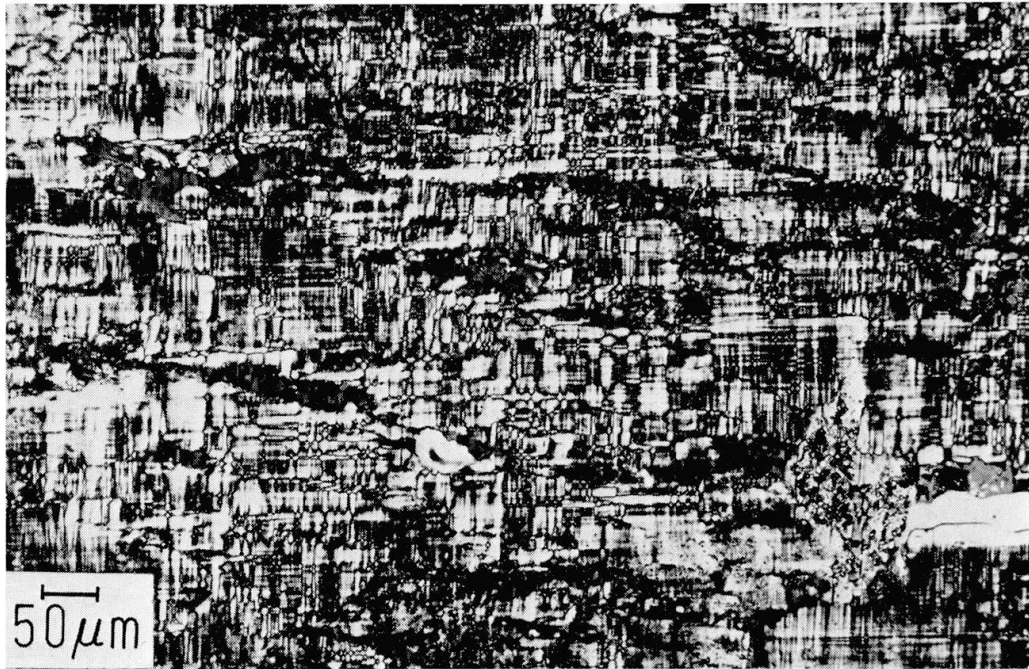


Fig. 3 Microcline perthite with distinct cross hatching (microcline twin law). Thin section oriented // (001). Phenocryst from Medel granite, Val Medel traverse, sample SZA 1853 (Table 3). Crossed polarizers.

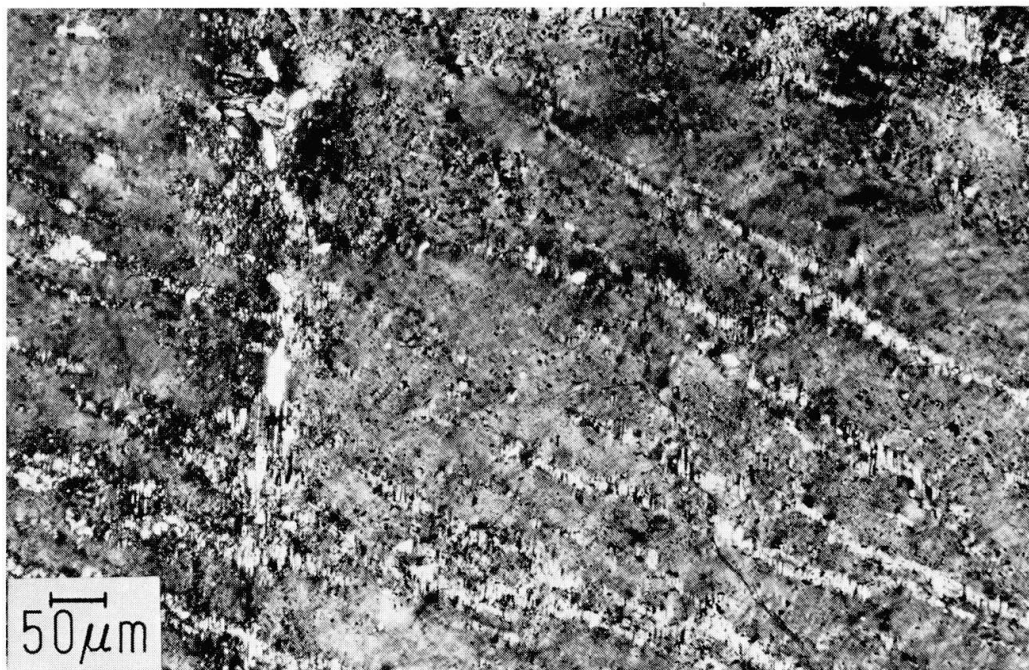


Fig. 4 Orthoclase perthite with monoclinic bulk optics of the K-feldspar and indistinct, patchy extinction, but no cross hatching visible. Thin section, the part at right is oriented // (001). Karlsbad twinned phenocryst from Medel granite, Val Medel traverse, sample SZA 1870 (Table 3). Crossed polarizers.

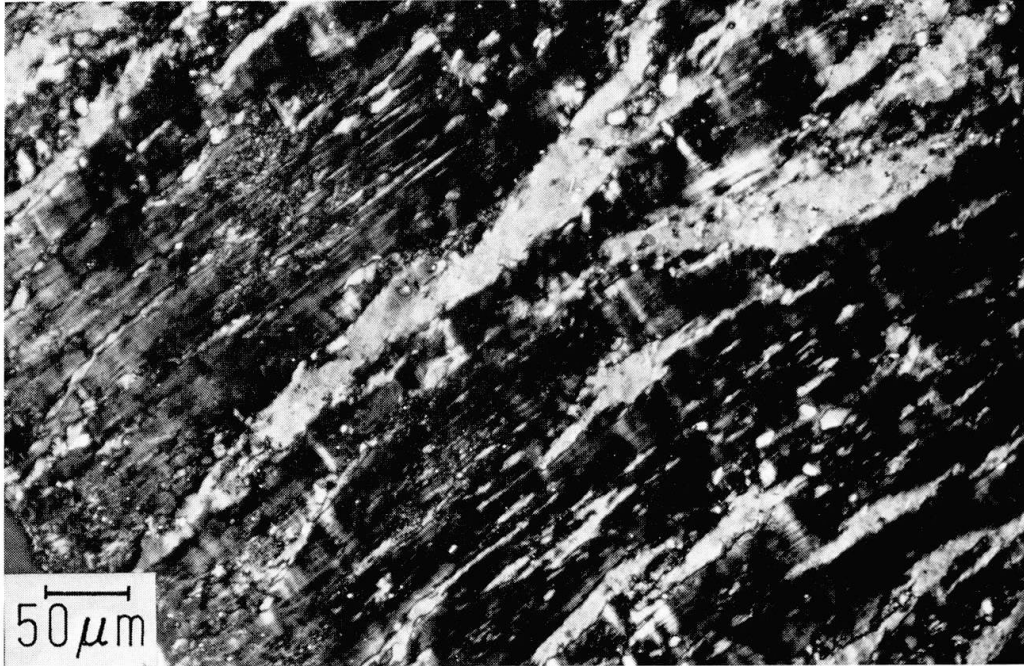


Fig. 5 Orthoclase perthite with local development of visible, very faint and blurred cross hatching in K-feldspar. Thin section oriented // (001). Phenocryst (or auge) from Gamsboden gneiss. High microcline region of the St. Gotthard traverse, sample GSS 7312 B (Gotthard highway tunnel, Table 2). Crossed polarizers.

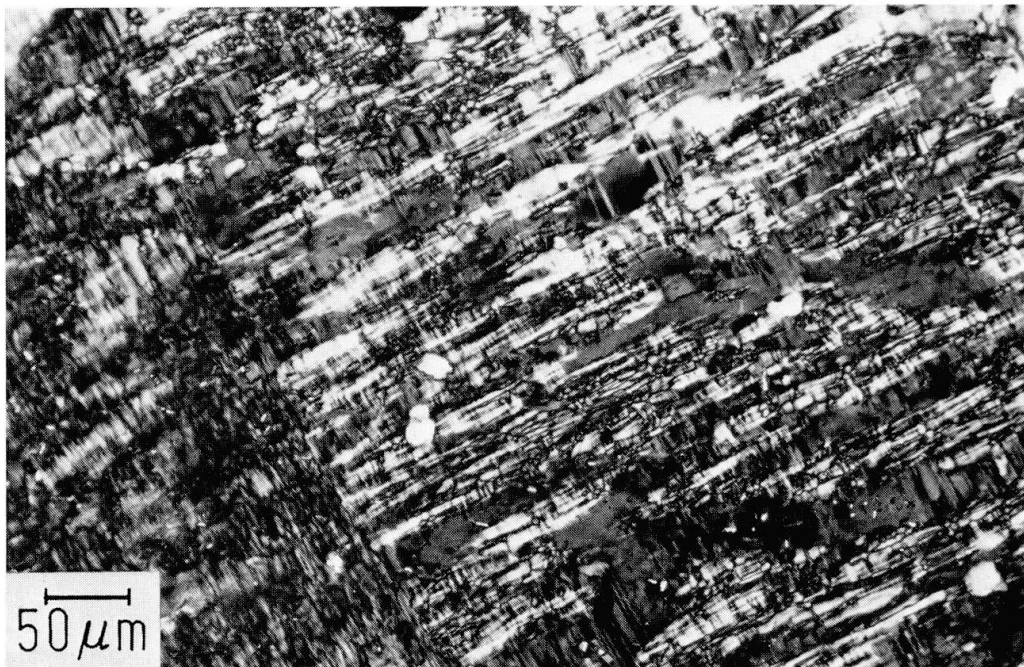


Fig. 6 Areas of orthoclase (medium grey, homogeneous) and microcline (with distinct cross hatching) and albite (also twinned) in perthite. Thin section, the part at right is oriented // (001). Karlsbad twinned phenocryst from central Aare granite, low microcline region of the St. Gotthard traverse, sample GPS 55 (Table 2). Crossed polarizers.

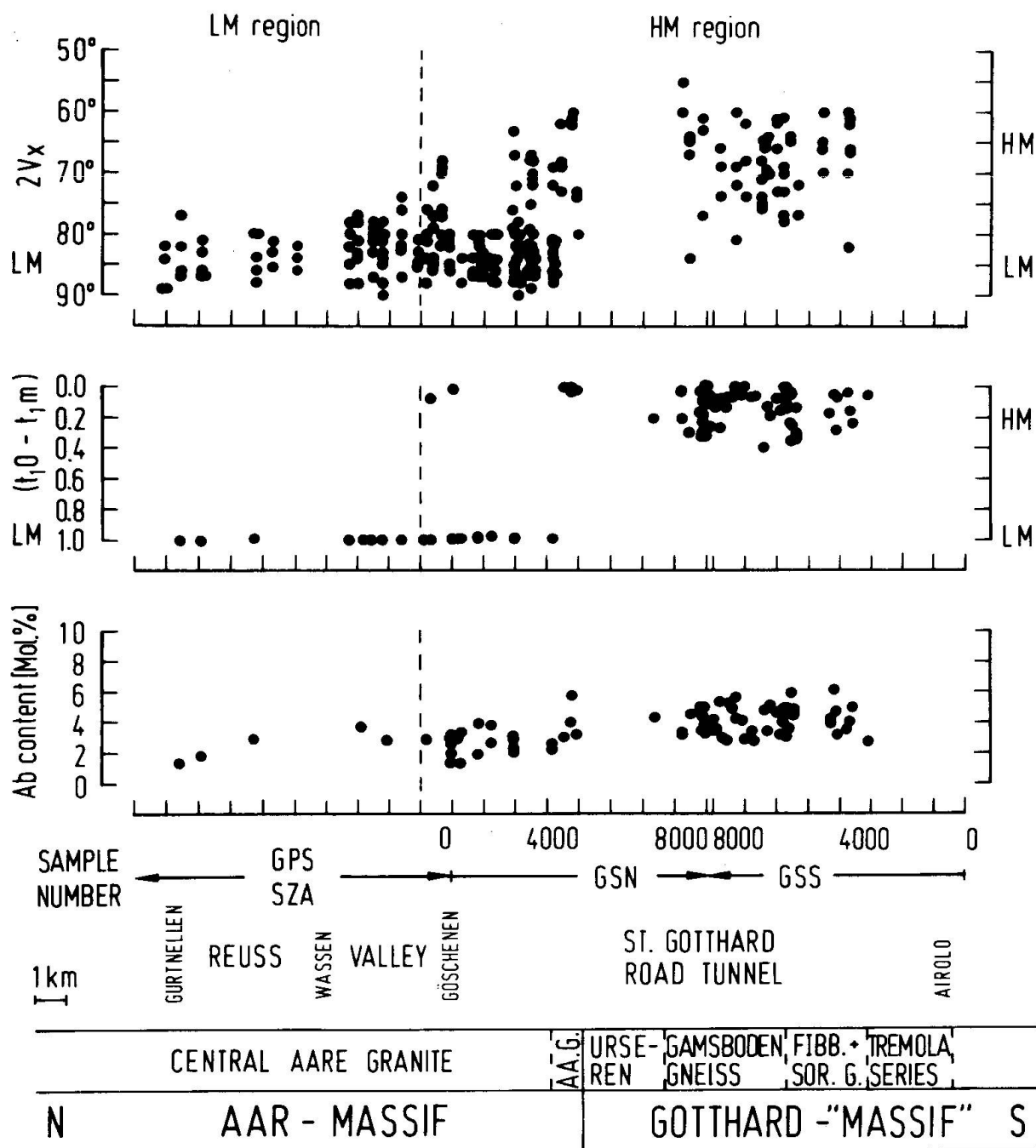


Fig. 7 Plot of optic axial angle $2V_x$, degree of Al,Si order and composition of K-feldspar of perthites along the St. Gotthard traverse (Table 2 and 4). The K-feldspar discontinuity is indicated by the first appearance of high microcline. HM = high microcline, LM = Low microcline.

lar patchy (Fig. 4), but also areas of locally developed very faint and diffuse cross-hatching may be observed (Fig. 5). Even the most homogeneous samples never reach the appearance of sanidine. The Na-feldspar in general tends to be smaller in its dimensions.

The very appearance of the K-feldspars (which in many cases is only observed on the U-stage) shows that they are no single crystals. Therefore, both

group names used above denote the microscopical appearance of *pseudomorphs*. From our experience we can predict that the K-feldspar of the microcline perthites in general has a structural state near low microcline, whereas the character of the orthoclase perthites is ambiguous: As will be shown in the following, their K-feldspar may exhibit various stages between high and low microcline.

Pseudomorphs showing the characteristic appearance of one of the two groups are very frequent, but more or less distinct transitions were observed, showing both types within the same pseudomorph (Fig. 6). Corresponding observations were made by HAFNER & LOIDA (1980) in the Rotondo granite. As far as the large phenocrysts or augen are concerned, Karlsbad twinning is very frequent irrespective of the special appearance described above.

The two groups of pseudomorphs show the following distribution along the St. Gotthard traverse. The location of the K-feldspar discontinuity (Fig. 7) which will be described in the following sections, will serve as a reference point. From the north to the south the amount of microcline perthite decreases, orthoclase perthites become frequent around the discontinuity, and their abundance further increases to the south. Also, the already mentioned transitional type composed of orthoclase⁴ and microcline perthite (Fig. 6) may be found in the north. On the other hand, grains of well developed microcline perthite are still found in the south together with the predominating orthoclase perthites. Occasionally, transitions between distinct and extremely diffuse cross hatching may be observed within the same grain.

Farther to the south, partial recrystallization of the K-feldspar can be observed and more or less homogeneous orthoclase⁵ perthites dominate. This is the reason why VOLL (1976) expected the K-feldspar discontinuity in the southern Gotthard, whereas Fig. 7 shows it amidst the Central Aare granite. This shows that the discontinuity cannot be inferred from pure microscopical observation of microcline perthite and orthoclase perthite in every case.

In the granitic rocks we occasionally observed newly formed accessory adularia, and without any regular distribution, more or less intensive formation of chess-board albite which, in some samples, may have fully replaced the K-feldspar.

⁴ It *always* has $2V_x$ angles of *low* microcline.

⁵ It *predominantly* but not *exclusively* has $2V_x$ angles of *high* microcline.

(b) Optical data of the K-feldspars

The extinction angle $X' \wedge (010)$ on (001) was found to be at maximum -17° to -18° in the well developed twin domains of the microcline, corresponding to the value of low microcline. Occasionally, it may decrease below -10° . The extinction of the orthoclase mostly is near zero, but increases as soon as cross hatching becomes visible. The optical axial angle, generally averaged over numerous twin domains, is always large and rather constant, mostly $2V_x = 80-88^\circ$ ($r > v$), in the distinctly twinned microcline. It always turns out to be low microcline.

The microscopical appearance of the more or less homogeneous orthoclase is ambiguous: In general, the optical axial angle is found in the range of $2V_x = 53-108^\circ$ ($r > v$, stronger with smaller angles). Its mean optical orientation appears monoclinic with O.A.P. $\perp (010)$. Further evidence for this ambiguity are frequently occurring optical inhomogeneities within the same grain: for instance $2V_x = 69^\circ$ and 83° (Central Aare granite, sample GSN 3150). Another example are orthoclase areas having $2V_x = 59-66^\circ$ within coarsely twinned microcline, similar to Fig. 6 (Medel granite, sample SZA 1876). Occasionally, both parts of Karlsbad twins show quite different axial angles, for instance part I: $2V_x = 73-83^\circ$, and part II: $2V_x = 55-57^\circ$. Also, "orthoclase" with scarcely visible, very faint cross hatching may even show axial angles as small as $2V_x = 66^\circ$.

It has been known long ago that K-feldspars showing the microscopical appearance of orthoclase may have axial angles corresponding to low microcline. For instance, MARFUNIN (1961) gives an upper limit of $2V_x \sim 84^\circ$ for the variation of optical *and* x-ray monoclinic K-feldspar. From the mere optical data it can be concluded that the orthoclase studied here corresponds to those described by GOLDSMITH & LAVES (1954, 1961), interpreted as cryptotwinned microcline of variable degree of order.

While the axial angle of the orthoclase was mostly found to be $2V_x < 86^\circ$, in some instances $2V_x = \sim 90-108^\circ$ was measured. These unusual large angles have been known long ago from the so-called iso-orthoclase (iso-microcline). New examples have been described recently by VOLL (1969) from the Dalradian of the Scottish Highlands, and by v. RAUMER (1967) from the Mont Blanc Massif. On the basis of detailed optical measurements, BLASI (1972) discussed iso-orthoclase from the Argentera Massif (Alpes Maritimes) as pseudomorphs, having a special internal texture. Most of all iso-orthoclases studied here were detected while searching for orthoclase with very small axial angles in the southern neighbourhood of the K-feldspar discontinuity (Fig. 7). The relevance of this local, high abundance of iso-orthoclase is still questionable.

A satisfying interpretation of iso-orthoclase is still pending. However, the K-feldspars with $2V_x \geq 90^\circ$ studied here do show more or less the same appearance as "normal" orthoclase with $2V_x < 90^\circ$. This is supported by $2V_x = 80^\circ$ and 95°

measured *within* the same grain. From their extinction one gets the impression of minute inhomogeneities which are no longer resolvable by the microscope. Also, they exhibit particular diffuse and often anomalously curved isogyres. The measured area was not always free of fine albite exsolutions, but this alone probably cannot explain the enlargement of the axial angle above 90° . Reference measurements of single, sufficiently large twin domains of microclines from pegmatites always gave $2V_x = 80\text{--}85^\circ$. This meets well the values given by MARFUNIN (1961) and NEIVA (1972). Microcline displaying such axial angles shows always maximal Al,Si order (DE PIERI 1979, STROB 1982). Therefore, we have no doubt that single crystals of K-feldspar show $2V_x < 85^\circ$, indeed. Larger axial angles presumably depend on the still unknown internal texture of the pseudomorphs called iso-orthoclase.

For the purpose of distinguishing between high and low microcline, we choose the frequency minimum near $2V_x = 75^\circ$ in Fig. 11 as boundary. If we compare this with the data given in literature, a K-feldspar having $2V_x < 40^\circ$ and O.A.P. $\perp(010)$, is expected to be a sanidine⁶ with high probability. Therefore, the smallest angle $2V_x = 53^\circ$ measured here, with $r > v$ and O.A.P. $\perp(010)$, may correspond to a weakly ordered high microcline.

The fairly sharp change in structural state along the St. Gotthard traverse, indicated by optical axial angles and lattice parameters (Fig. 7), is referred to as the *K-feldspar discontinuity*. We recognize a northern low microcline region and a southern high microcline region displaying a considerable scatter of structural states. Since we tried to particularly find orthoclase with the small $2V_x$ of high microcline in our samples, the frequency of low microcline presumably is higher than it may be expected from Fig. 7. It will be shown later, that the frequency minimum near $2V_x = 75^\circ$ is not incidental.

In many respects the pattern of Fig. 7 is analogous to the findings of STEIGER & HART (1967), WRIGHT (1967) and VOLL (1969).

(c) Composition and Al,Si distribution of the alkali feldspars

The composition of K-feldspar of the perthites both from Aar and Gotthard Massif varies between $\text{Or}_{98.5}\text{Ab}_{1.5}$ and $\text{Or}_{93.5}\text{Ab}_{6.5}$ (Table 4 and 5). As can be seen from Fig. 7, the average Ab content within the low microcline region is somewhat lower than within the high microcline region. The lattice parameters of

⁶ After LAVES & VISWANATHAN (1967) the sanidine/microcline boundary lies between $2V_x = 43\text{--}63^\circ$ (the largest angle belonging to single crystals with stable Al,Si distribution); after MARFUNIN (1961) $2V_x < 43^\circ$ indicates sanidine. More recently, this boundary is drawn by SMITH (1974, I) near 55° , by STEWART (1975) near 50° , by NEIVA (1974) near 58° , and by DE PIERI (1979) near $45\text{--}40^\circ$.

K-feldspar show a considerable variation between the maximum triclinicity of low microcline and monoclinic values, with a marked gap in between. Since there are no significant differences between both traverses, all data were plotted together in Fig. 8 and 9.

The exsolved plagioclase of perthites unaffected by metasomatic alteration is estimated <20 vol%. As far as both traverses are concerned, composition and structural state of the Na-feldspar are close to the low albite end-member.

The calculated Al,Si distributions of the K-feldspar are plotted in Fig. 10. It is clearly demonstrated that the microcline series obviously has no connection to the "theoretical low sanidine" with $2t_1-2t_2 = 1.0$ and $t_1 = 0.5$ (LAVES 1960). It may be extrapolated formally to a considerably less ordered monoclinic K-feldspar. We expect the critical Al,Si distribution of the transition of "true low sanidine" to high microcline at T_{diff} close to $2t_1-2t_2 \sim 0.4$ and $t_1 \sim 0.35$ in accordance with Fig. 15 (also compare HAFNER et al. 1962, BERNOTAT 1979, and KROLL 1980b). The data of GUIDOTTI et al. (1973), DORA (1976), and of parts II to IV of

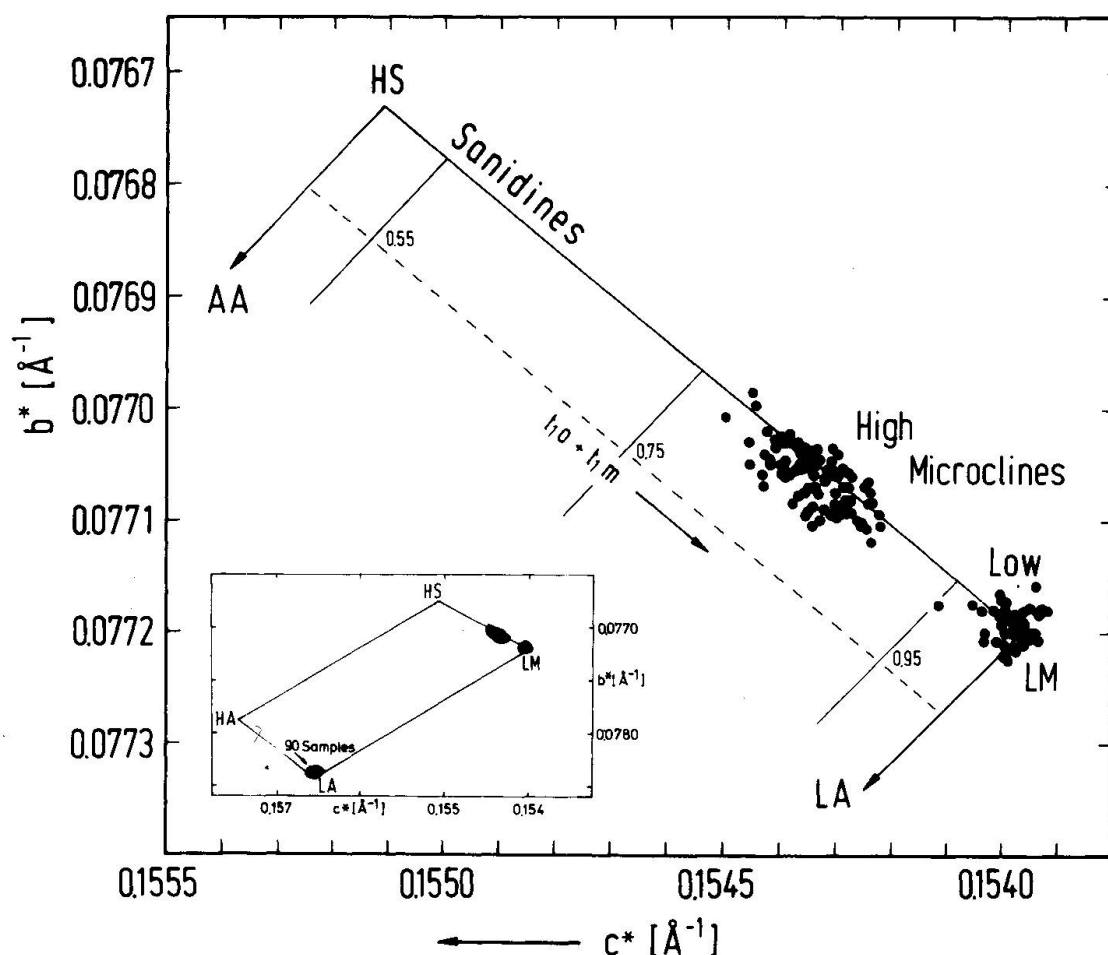


Fig. 8 b^* , c^* - plot of perthitic alkali feldspars from the St. Gotthard and Val Medel traverses (Table 4 and 5). AA = analbite, LA = low albite, HS = high sanidine, LM = low microcline.

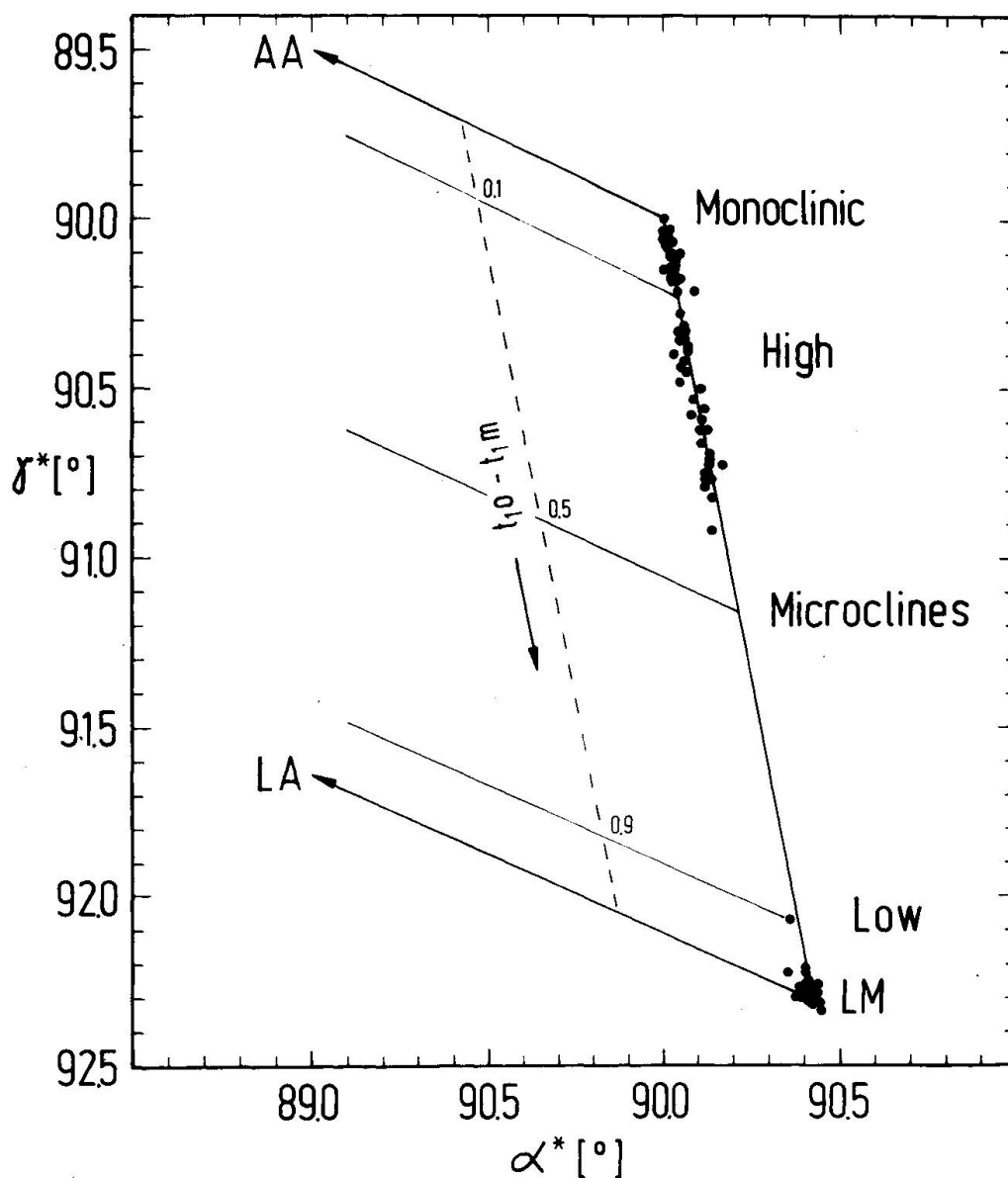


Fig. 9 α^* , γ^* - plot of perthitic alkali feldspars from the St. Gotthard and Val Medel traverses (Table 4 and 5). Symbols as in Fig. 8. All Na-feldspars plot as LA.

this series of articles fit well into Fig. 10. This pattern is probably characteristic for regional metamorphic series. But low hydrothermally grown adularia may behave distinctly different (BAMBAUER & LAVES 1960, BERNOTAT & NIEDERMAYER 1980).

The well known, sensitive splitting of the powder interferences 131/1 $\bar{3}$ 1 may allow to distinguish more than one triclinicity within a K-feldspar grain. A few samples gave a monoclinic powder diagram with one broadened 131 interference, indicating insufficient resolution of high (?) microcline with α and γ near 90°.

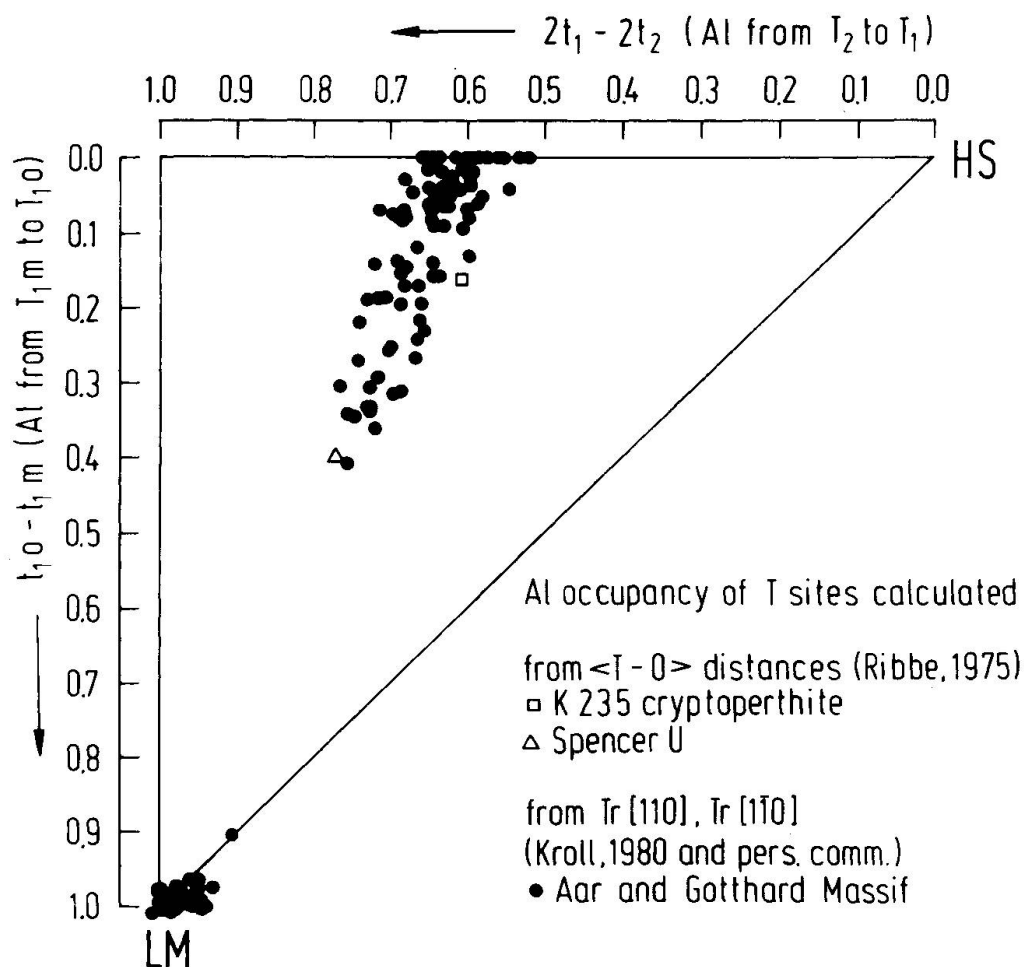


Fig. 10 Al-site occupancies in K-feldspar of perthites, calculated by the method of KROLL (1980a). St. Gotthard and Val Medel traverses (Table 4 and 5). For comparison, data of samples K 235 and Spencer U, given in Table 6, are plotted. Symbols as in Fig. 8.

From the monoclinic lattice parameters mentioned above Al,Si distributions were calculated formally. They plot in Fig. 10 on the line with $t_{10} - t_{1m} = 0$ near $2t_1 - 2t_2 \sim 0.6$. A comparison of Fig. 13 with Figs. 11 and 14 shows that no sanidine was found. The finding of metrical monoclinic K-feldspar may be explained by the already mentioned internal texture of orthoclase. We have to consider a size of microcline domains beyond the resolution limit of the Guinier method. For such x-ray monoclinic orthoclase MARFUNIN (1961) gave an upper limit of $2V_x \sim 84^\circ$ (corresponding to $2V_x$ of low microcline). Also, HAFNER & LAVES (1957, 1963) studying similar K-feldspars, with $2V_x = 49-79^\circ$, O.A.P. $\perp(010)$, by using IR and NMR spectroscopy, found evidence for an Al,Si order different from sanidine. Meantime, the direct proof for the submicroscopical domain texture of an orthoclase by means of high resolution TEM is given by EGGLETON & BUSECK (1980). Nevertheless, they also imaged small, apparently

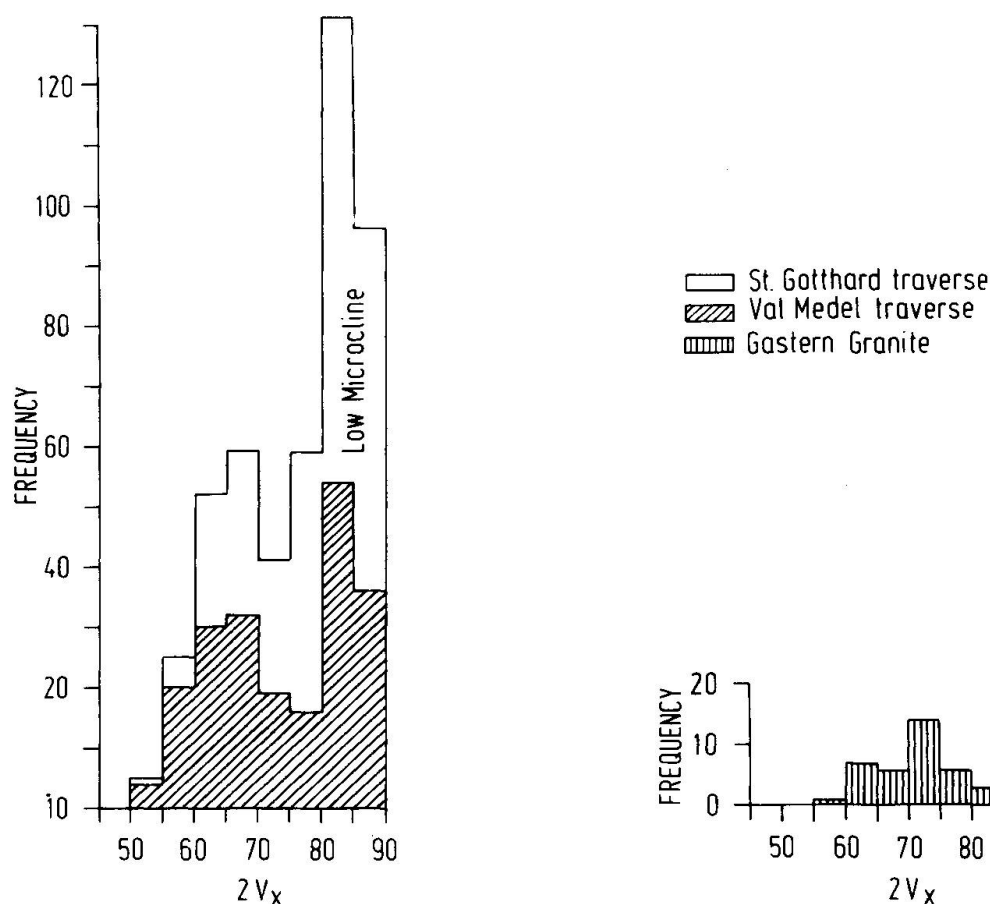


Fig. 11 Histogram of the optic axial angle $2V_x$ (Table 2 and 3) of K-feldspars from the St. Gotthard and Val Medel traverses.

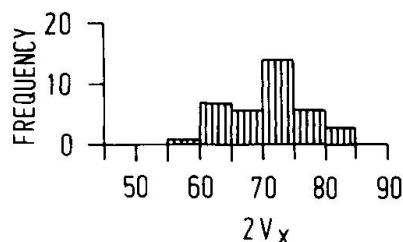


Fig. 12 Histogram of the optic axial angle $2V_x$ of K-feldspars from the Gastern granite, northwestern Aar Massif (GYSIN 1948).

monoclinic areas besides finely twinned triclinic domains. We suppose that the monoclinic K-feldspars found here, in reality, have $t_{1o} - t_{1m} \neq 0$.

The gap in the range of structural states between high and low microcline shown in Fig. 10 is apparently not incidental. A comparison of Figs. 11, 13, and 14 shows that similar results may be achieved by different, independent methods. This confirms earlier histograms on the basis of the triclinicity Δ , using samples of quite different origin (DIETRICH, 1962), samples from metamorphic rocks of the Massif Central, France (MERGOIL-DANIEL 1970), and from the region of highest metamorphic grade within the Lepontine Alps (Hiss, 1979). Comparable results were obtained on igneous K-feldspar megacrysts by EGGLETON (1979), on K-feldspars from quite different metamorphic regions by GUIDOTTI et al. (1973), and by BERNOTAT & MORTEANI (1982). Because the intermediate structural states are relatively rare, we only use the terms high and low microcline. Compare Figs. 8 and 9 to Fig. 15, where the relation between the lattice parameters and the diagram of the Al,Si-order can be understood qualitatively (p. 220).

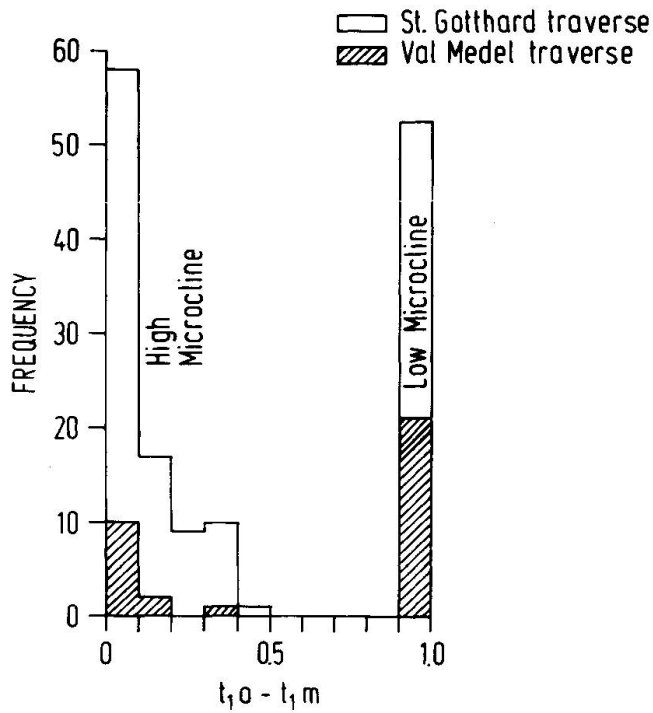


Fig. 13 Histogram of the degree of Al,Si order (plotted in Fig. 10) of K-feldspars from the St. Gotthard and Val Medel traverses.

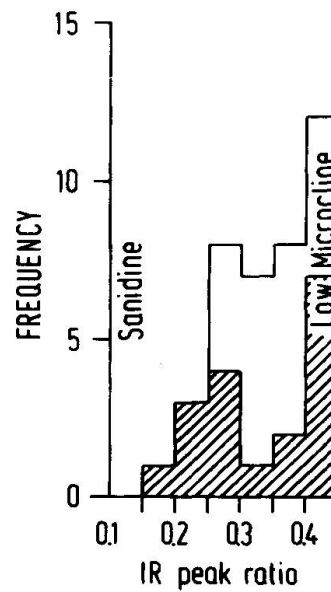


Fig. 14 Histogram of the ratio a/b of the infrared absorption bands at about 650 and 590 cm⁻¹ (according to Fig. 10 A of HAFNER and LAVES 1957) of K-feldspars from the St. Gotthard and Val Medel traverses.

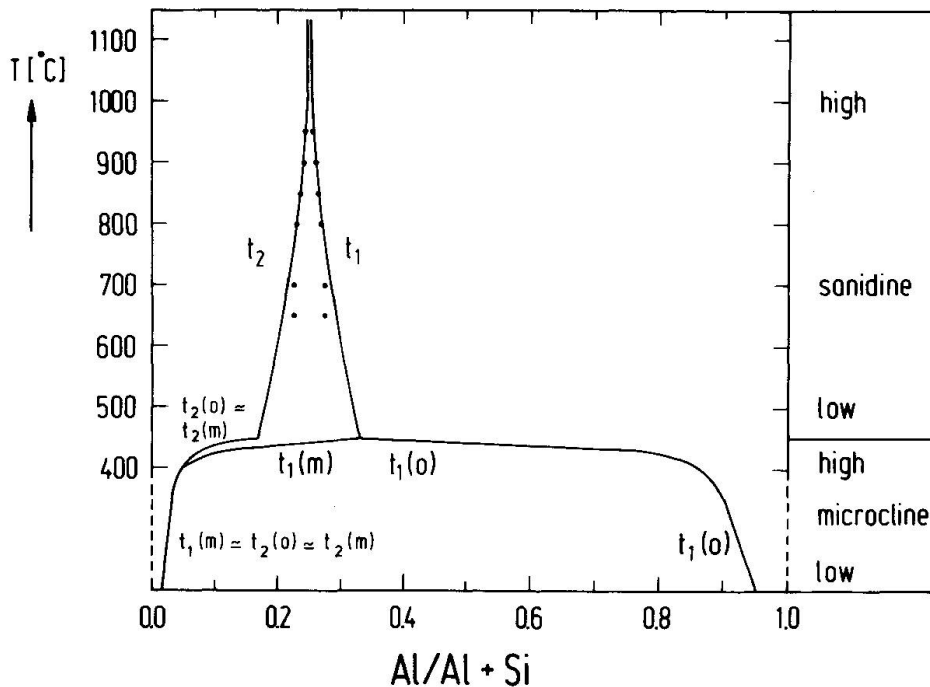


Fig. 15 Schematic diagram of the Al,Si distribution for K-feldspar. Al-content of the two and four non-equivalent T sites, respectively, under equilibrium conditions as a function of temperature. Modified after LAVES (1960) by KROLL (1971). Dots: experimental data. Temperatures below 400°C were omitted.

The Al,Si distributions plotted in Fig. 7 were calculated from lattice parameters with one exception. The northernmost high microcline point represents a K-feldspar pseudomorph which contains a small amount of high microcline besides low microcline. The number of high microcline lines was not sufficient for refinement of lattice parameters. Its structural state was estimated from a few line positions. Some samples irregularly distributed within the "low microcline region" showed very weak additional peaks between the 131 and the $1\bar{3}1$ peak. This indicates minor traces of high microcline since oligoclase is not present. However, high microcline was not detected by optical methods in any of these samples. The scatter of x-ray data in Fig. 7 is small as compared to $2V_x$. There probably exist smaller amounts of variable structural states which cannot be found on the x-ray powder diagram. The optical measurements allow a better resolution of local differences. But the strong diffusiveness of the isogyres indicates that $2V_x$ is an average of different states even in the smallest measurable volume.

(d) Infra-red data of the K-feldspars

The frequency of the intensity ratio of two characteristic absorption bands is shown in Fig. 14. The analogy to the histogram of $2V_x$ (Fig. 11) is obvious: Sanidine is not detectable and the minima of both distributions at intermediate structural states is demonstrated for both traverses.

Discussion

(a) Is K-feldspar a geological thermometer?

There is no doubt that the Al,Si distribution of alkali feldspars is governed essentially by temperature. But certain degrees of order may be used as geological thermometer only, if they represent states of equilibrium and can be recognized as such. As an additional condition it must be sure that the state considered was quenched to low temperature without delay.

While the ordering behaviour of Na-feldspars and sanidines is rather well known above 700°C, quantitative informations are lacking for microcline. The reason for this is the extremely sluggish attainment of equilibria at low temperatures under experimental as well as natural conditions. Therefore, only the upper part of the ordering diagram shown in Fig. 15 is derived from experimental data. On the basis of structure refinements and reasonable estimates of temperatures, the lower part of the diagram, i. e. below 500°C, neglecting details, is thought to describe the ordering behaviour reasonably well. It should not be

used for temperature estimates. The nearly ubiquitous microcline twinning and other mimetic domain fabrics prove that K-feldspars primarily grow as sanidine (LAVES, 1950), irrespective of the given conditions. Apparently, exceptions are rare. This was discussed in some detail by GOLDSMITH & LAVES (1954) and BAMBAUER & LAVES (1960). The diffusive transformations of K-feldspar and Na-feldspar⁷) differ from each other, since, as a result of the transition sanidine → microcline, triclinic domains must form within a monoclinic host. From this process results a high kinetic barrier. Resulting from lattice distortion and twinning during the development of the triclinic domains (compare Fig. 8 of LAVES, 1950), the internal energy released by the ordering process will be used up again as strain and domain-boundary energy. This is independent of whether we assume the primary formation of "nuclei" (GOLDSMITH & LAVES, 1954) or of "transverse waves" (McCONNELL, 1971). EGGLETON & BUSECK (1980) have shown by high resolution TEM that monoclinic and triclinic, continuously strained, or twinned domains even may occur side by side within volumes of approximately 2×10^3 elementary cells. They calculated that transformation energy released and strain energy stored have a similar order of magnitude. Eggleton & Buseck believe that this is the reason for the strong trend to metastable, intermediate states of order. Indeed, two processes very sluggish at low temperatures are expected to take place simultaneously during the further development of domains to a (hardly ever reached) single crystal of low microcline: Further release of transformation energy with increasing Al,Si order and lowering of the stored boundary energy by progressive growth of the microcline domains. While the ordering of Na-feldspar was found to be relatively fast, the ordering of K-feldspar is expected to be much slower. According to this, SIPLING & YUND (1974) and YUND & TULLIS (1980) found that the corresponding activation energy of K-feldspar is noticeable higher than that of Na-feldspar. It is supposed that the sluggishness of the domain growth essentially is the retardation factor. Therefore, it seems thermodynamically plausible that no maximum Al,Si order can be attained as long as microcline domains are three-dimensionally strained by their neighbour domains. Up to now this barrier has not been overcome successfully by experiments. The orthoclases and microclines (as defined in Table 1) show the resulting metastable, mimetically twinned domain texture of transition pseudomorphs after sanidine. Experimental investigations of the kinetics of ordering by YUND & TULLIS (1980) have confirmed the old experience that "catalytical" influences (as compiled by BAMBAUER, 1966 and MARTIN, 1974) apparently were necessary to accelerate the processes mentioned above. They especially pointed out that, at a given temperature, H₂O pressure is the principal accelerating factor besides increasing Na/K ratio and mechanical deformation.

⁷ Analbite (trcl.)/albite (trcl.); pure monalbite only exists above $T_{\text{diff}} = 980^\circ\text{C}$.

As can be seen from the literature cited in the introduction and, very clearly, from the results of this paper, strong inhomogeneities with respect to metastable structural states are very common among the alkali feldspars from the Central Swiss Alps. Furthermore, we do not know at all whether and at which time an equilibrium between Al,Si distribution and temperature of metamorphism was attained. Therefore, the attempt of HISS (1978) to directly use Al,Si distributions to determine temperatures of formation (!), seems to be unreasonable. In addition, the STEWART & WRIGHT (1974, Fig. 6) diagram used by HISS, having the same aim as Fig. 15, has been qualified as schematic only by the authors.

Up to now there is no answer to the question, at which temperature a given Al,Si distribution of a natural microcline was frozen in. As will be shown in the next section, the kinetical barrier inherent to the diffusive transformation of K-feldspar may be used itself as an indicator of temperature.

(b) The K-feldspar discontinuity

As has been mentioned before, the pattern of Fig. 7 may be characteristic for contact metamorphic as well as regional metamorphic series of K-feldspars. Taking the work of STEIGER & HART (1967) and VOLL (1969) into account, an interpretation of the Alpine K-feldspar discontinuity is attempted in the following.

Since there are no usable experimental data on Al,Si ordering in the temperature range of 600–300°C relevant to this discussion, the argumentation is depending on extrapolations from experiments, on observations in the field, petrological data, and the present knowledge of the structural behaviour of alkali feldspars. Following the review of the metamorphic zonation along the St. Gotthard traverse by FREY et al. (1980), a fairly regular temperature/pressure gradient existed at the climax of the mid- to late tertiary metamorphism, ranging from at least 300°C at the northern end of the Aar Massif to at most 550°C at the southern end of the Gotthard. The pressures were around 2–3 Kbars, and the fluid phase within the pores of the different granitic rocks apparently had a quite similar composition. The raising of temperature was obviously slow and continuous. The recrystallization of the mineral constituents became more intense with increasing temperature and pressure to the south. It is essentially syn- and posttectonic with respect to the Alpine deformation. The feldspars, brittle at temperatures below 450–500°C, show distinct recrystallization in the southern Gotthard (VOLL, 1976). During the following retrograde phase with a relatively steeper decrease of temperature⁸, the high temperature part of the tra-

⁸ So far, there are only insufficient informations on the temperature/time relation available for the Aar Massif and the Helvetic Nappes; the data available for the Lepontine area are still incom-

verse fell below 300°C not much earlier than 15 m. y. ago. Probably, the temperature T_{diff} of the sanidine/microcline transformation (between 500 and 400°C) was passed during a period of faster cooling at about 20 m. y. ago, thus providing more favourable conditions for the quenching of structural states.

In the following the history of structural states of K-feldspars along the St. Gotthard traverse will be considered as a function of temperature (and pressure) and time. Of course, the initial, pre-Alpine states are not known. If we choose the state of a high microcline (see below p. 223), then, two cases have to be considered: heating a rock to temperatures $T < T_{\text{diff}}$ and to $T > T_{\text{diff}}$; the value of T_{diff} will be estimated in the last section. We discuss both cases in regard to the ordering diagram (Fig. 15). The diagram shows the following sections to be distinguished for kinetic considerations:

- (a) high to low sanidine, showing a small Al,Si change within a very broad range of temperatures;
- (b) transition sanidine \rightleftharpoons microcline;
- (c) high microcline with approximately $0.45 < t_{10} < 0.85$, showing a great Al,Si change within a very narrow range of temperature;
- (d) low microcline with approximately $t_{10} > 0.85$, showing small Al,Si changes (presumably smaller than shown in the diagram) within a broad range of temperatures.

The influence of Ab content should not be neglected.

(1) $T < T_{\text{diff}}$. The most frequent case to be expected is: Heating of a perthitic high microcline displaying a metastably fixed *degree of order* corresponding to section (c) from low temperatures (given by its depth of that time) to *temperatures* above 300°C and corresponding to (d). VOLL (1969) deduced from his field observations that even at temperatures near 300°C high microcline must have changed to fully ordered low microcline. Also, further exsolution of albite should have proceeded. On the other hand, SIPLING & YUND (1979) argued from the extrapolation of their kinetical data that ordering is unlikely at such low temperatures. Perhaps, this very far extrapolation is not allowed. We believe that the results of STECK & BURRI (1971) and VOLL (1976), confirming VOLL (1969), are sufficiently relevant to join their opinion. If the presence of fluids and the influence of local stress on the mineral constituents during geological time is taken into consideration, a recrystallization of the fine microcline domains and an approach to equilibrium order might be expected.

Minor traces of high microcline, only occasionally detected in the low microcline zone, are assumed to be relics. They indicate that maximum Al,Si order has not always been reached.

plete. WERNER (1980) made different model calculations for a temperature maximum at about 30 m. y., whereas FREY et al. (1980) considered a temperature above 500°C between 40–20 m. y.

As a variant of this case the hydrothermal growth of metastable sanidines within the stability range of microcline has to be accounted. Adularia formed in this way is extensively distributed over the Central Alps.

(2) $T > T_{\text{diff}}$. After having passed T_{diff} upon heating, the mixed crystal will contain about 10 mol% Ab. The mixed crystal will be transformed to sanidine with some delay because domain boundaries and regions of short range order have to be destroyed and thus disorder will increase. With further increase of temperature the sanidine becomes richer in Ab until a homogeneous mixed crystal is formed. During the following retrograde phase this process runs in the opposite direction. Then, when passing T_{diff} , the kinetic barrier mentioned becomes effective. Adaption of Al,Si distribution to temperature will be delayed and early formed microcline domains will be retained. If catalytic influences are lacking, freezing of this state will result in pseudomorphs of orthoclase perthite. The development of Na-feldspar exsolutions, neglected here to some extent, has been thoroughly discussed by LAVES & SOLDATOS (1963).

For the following discussion we assume that Fig. 15 represents equilibrium states of order. Then, regarding delay and overheating of the prograde transformation to sanidine, the metastable ordering paths are expected to lie *above* the equilibrium paths (compare LAVES, 1960 and LAVES & VISWANATHAN, 1967). The disordering process will run the slower, the closer the temperature to T_{diff} was, and the coarser the domains of the primary microcline were. If homogenization did not reach completeness during the prograde phase, the K-feldspar will keep a "memory" of the former state, and growth of new domains during the retrograde transformation to microcline will be eased. Therefore, among a comparable series of K-feldspars, those which were heated to the highest temperatures should develop the finest domains upon cooling and thus probably will preserve best the state of high microcline.

Regarding delay and undercooling of the retrograde transformation to microcline, the metastable ordering paths are expected to lie *below* the equilibrium paths (compare also BAMBAUER & LAVES, 1960).

It may be assumed from Fig. 10 that the microcline series originated from a "true low sanidine" with $2t_1 - 2t_2 < 0.4$, and $t_1 < 0.35$, resp., as predicted in good agreement by Fig. 15. In addition, the observed ranges of the structural states plotted in Fig. 10 are fitting into different sections of Fig. 15: $0 < t_{10} - t_{1m} < 0.4$ (fig. 10) is located between $\sim 0.35 < t_{10} < \sim 0.60$ of section (c), and the other one at $t_{10} - t_{1m} < 0.9$ (Fig. 10) is located at $t_{10} < 0.9$ of section (d). This was expected from the preceding discussion. It may be assumed that the frequency minima at intermediate degrees of order, shown in Figs. 11, 13, and 14, are a result of different ordering kinetics. Of course, a definitive prove could not be given here. These findings apparently are not incidental. ČERNÝ & MACEK (1974) made analogous observations on K-feldspars from a pegmatite.

From the discussion given above, the pattern of Fig. 7 may be interpreted in

the following way. During the prograde phase of the Lepontine metamorphism the P/T gradient was moving from the south to the north⁹ and gave rise to the formation of new Al,Si distributions and solid solutions of the pre-metamorphic K-feldspars. We have to imagine a zone of approaching low microcline with $T < T_{\text{diff}}$ moving to the north which was followed by a sanidine zone with $T > T_{\text{diff}}$. During the retrograde phase the present high microcline zone arose from the sanidine zone. Thus, the K-feldspar discontinuity is believed to mark the northermost point of the traverse, at which T_{diff} was reached. Thereby a *microcline/sanidine transformation isograd* may be defined. However, some limitations are to be taken into account. The discontinuity is expected to be particularly sharp if the metamorphic gradient was steep, the isothermal surface T_{diff} was perpendicular to the traverse, and an equilibrium microcline/sanidine was quenched. In this ideal case it might be possible to decide whether the transformation is of first or higher order. In reality the northermost point T_{diff} and the K-feldspar discontinuity will not exactly coincide. Obviously the kinetics of the transformation microcline \rightarrow sanidine should be slowest just above the temperature of transformation, and probably T_{diff} was reached at the northermost point for a relatively short time only. Hence it seems likely that during metamorphism a more or less distinct zone of incomplete disordering formed southward of the northermost point. A modification of this might have happened during the retrograde transformation sanidine \rightarrow microcline: sanidines still containing "nuclei" of microcline due to incomplete transformation might transform faster than homogeneous sanidines. Furthermore the width of this zone of disequilibrium is related to the dip of the isothermal surface T_{diff} . The gentle slope, shown by $2V_x$ at the discontinuity between Göschenen and Wasen, might be indicative for the existence of this zone. Irrespective of the interpretation given above, it has to be kept in view that the metastable state of high microcline may completely break down due to catalytic activities at any point of the traverses discussed here. A well known example is the local formation of low microcline in shear zones.

Probably, the distinctness of the discontinuity also depends on the pre-metamorphic structural state of the K-feldspar. If we assume it to be high microcline, more or less abundant relictic high microcline might have survived in the Alpine low microcline zone with $T < T_{\text{diff}}$. A better contrast is to be expected from pre-metamorphic low microcline.

The essentials of this interpretation of the K-feldspar discontinuity may be also applied to the other traverses studied in the Swiss Alps (part II) and the Tauern Window (part III).

Apparently, the disordering of K-feldspar southward of the discontinuity was not necessarily accompanied by intense recrystallization as was shown by

⁹ On the basis of the presently exposed surface.

VOLL (1969) for a corresponding situation in the Scottish Highlands. A "recrystallization isograd" was found by VOLL (1979) farther to the south, near to the southern border of the Gotthard. A K-feldspar discontinuity will be formed only if a series of K-feldspars was sufficiently long heated in a gradient $T_1 < T_{\text{diff}} < T_2$. A steady cooling from approximately constant temperatures $T > T_{\text{diff}}$ along the whole traverse should not yield a discontinuity; the same holds for $T < T_{\text{diff}}$, as long as kinetics allow further ordering. On the other hand, different structural states may result from different cooling *rates* along a traverse with initial temperatures $T > T_{\text{diff}}$ (KROLL, 1980b). In fact, the Lepontine area cooled faster than the Aar Massif (WAGNER et al., 1977), but an additional influence on the discontinuity has not yet been observed.

Nothing is exactly known about the pre-Alpine structural state of the K-feldspars affected by Lepontine metamorphism. The state of the K-feldspars from the northern Aar Massif, which remained below 300°C, may be taken as a clue. For instance, the K-feldspars from the Gastern-Lauterbrunnen-Innertkirchen granite zone are usually preserved as orthoclase with a triclinicity $\Delta = 0$ (STECK & BURRI, 1971). The histogram given in Fig. 12 (GYSIN, 1948) indicates intermediate structural states, frequently found in granites (RIEDERER, 1965). This is confirmed by the variation of $\Delta = 0.06-0.85$ given by SEEMANN (1975) for the Punteglias granite, and $\Delta = 0$ and 0.70 given by WÜTHRICH (1965) for the Erstfeld gneiss.

(c) Estimate of the microcline/sanidine transformation temperature, T_{diff}

While KROLL et al. (1980) experimentally determined $T_{\text{diff}} = 978^\circ\text{C}$ for Na-feldspar, a corresponding accurate value cannot be given for K-feldspar. Three kinds of findings may provide an estimate of T_{diff} .

(1) Experimental data: the value $T_{\text{diff}} < 525^\circ\text{C}$, often cited after GOLDSMITH & LAVES (1954), only means that below this temperature no sanidine could be prepared from microcline (as starting material) during hydrothermal runs. The preparation of synthetic, intermediate microcline, reported by TOMISAKA (1962) could not be reproduced by SIPLING & YUND (1974). These authors suspected that TOMISAKA's results were due to homogenization of perthites. EULER & HELLNER (1961) were the first ones to show that nearly pure K-feldspars of adularia habit, prepared hydrothermally at 500°C and $P_{\text{H}_2\text{O}} = 1$ Kbar, displayed a very weak triclinicity ($2V_x = 50-52^\circ$). Until further experiments are at hand, we adopt $T_{\text{diff}} \sim 500^\circ\text{C}$ for pure K-feldspar.

(2) Theoretical considerations: HOVIS (1974) calculated the following temperatures of diffusive transformation from thermodynamical data: $P = 1$ bar, $T_{\text{diff}} = 451 \pm 47^\circ\text{C}$; $P = 5$ Kbar, $T_{\text{diff}} = 460 \pm 47^\circ\text{C}$.

(3) Petrological observations: STEIGER & HART (1967) got as a "best value" $T_{\text{diff}} = 350-400^\circ\text{C}$ from heat flow calculations (based on several assumptions)

at a granite contact. Another estimate by WRIGHT (1967) gave $T_{\text{diff}} = 375^{\circ}\text{C}$ for a mixed crystal $\text{Or}_{95}\text{Ab}_{05}$. VOLL (1969), also studying a granite contact showing a particular sharp K-feldspar discontinuity, estimated $T_{\text{diff}} = 420 \pm 20^{\circ}\text{C}$. On the other hand, he was able to extrapolate the boundary of first appearance of "monoclinic" K-feldspar near to the oligoclase-in boundary at approximately 500°C . VOLL (1976) assumed both boundaries close to the southern border of the Gotthard. Also, RAASE & MORTEANI (1976) found both boundaries to be "approximately conformable".

The K-feldspar discontinuity of the St. Gotthard traverse was found amidst the zone between the green biotite-in and the staurolite-in boundary for which FREY et al. (1980) give mean values of 450°C and 3 Kbar for the climax of the prograde metamorphism. The oligoclase-in boundary, which WENK (1962) and WENK & KELLER (1969) assumed to be located within the southern section of the Gotthard "Massif", was located by STECK (1970) on the basis of detailed microprobe work near to its northern border. This position is about 7 km south of the discontinuity, half-way to the staurolite-in boundary. Therefore, an assumption of 500°C seems too high for the discontinuity. The contact metamorphic temperature of 430°C , deduced by VOLL (1969) from the close vicinity to the cordierite boundary, seems to be the "best value" of temperature estimates for the discontinuity published up to this date.

Microcline may take about 10 mol% Ab maximally into solid solution. According to Fig. 7 microcline still contains approximately 5 mol% of unexsolved Ab at the discontinuity. If we consider the influence of pressure (HOVIS, 1976), $T_{\text{diff}} \sim 450^{\circ}\text{C}$ seems to be acceptable for a pressure of 3 Kbar and for a composition of $\text{Or}_{95-90}\text{Ab}_{05-10}$. The question whether K-feldspar undergoes a transformation of first or of higher order like Na-feldspar (KROLL et al., 1980; KROLL, 1980b) remains open. Comparison with pure K-feldspar shows a decrease of T_{diff} with increasing Ab content. This is in accordance with MACKENZIE & SMITH (1961), SMITH (1974, I, Fig. S-1) rather than with LAVES (1960) and LAVES & GOLDSMITH (1961).

(d) Practical aspects

To facilitate the tracing of a microcline/sanidine isograd on the basis of the K-feldspar discontinuity, some practical aspects are to be considered.

(1) The general characteristics of the type and degree of metamorphism within the region studied should be known, especially the direction of temperature gradients. If we take a hypothetical case for the Lepontine area in which we assume an increase of temperature to only $T < T_{\text{diff}}$, then we might expect a low microcline zone in the south and a pre-metamorphic high microcline zone in the north. This would result in a kind of discontinuity which we expect in the northern section of the Aar Massif. The example also demonstrates that one

should not rely on data from broadly scattered localities, especially in cases of different rocks with a different geological history. Better informations are provided by traverses with closely spaced sampling localities which should be traced parallel to the expected temperature gradient.

(2) To discover the true location of the K-feldspar discontinuity, representative sampling and sensitive methods of determination are required. Minor amounts of high microcline may be easily overlooked among prevailing low microcline. From our experience, we recommend a *combination* of x-ray, optical, and infra-red methods together with microscopical inspection of thin sections.

(3) As was shown, the distinction between «monoclinic» and triclinic K-feldspars by microscopical inspection or x-ray methods does not necessarily result in the detection of the K-feldspar discontinuity. But it is assumed that local accumulation of x-ray monoclinic orthoclase might bear additional genetic information. However, we do not yet know whether accumulations of such orthoclases in the Lepontine area (H. R. WENK, 1967; HISS, 1979) may reflect local peculiarities of the metamorphic history.

(4) The essential tectonic elements of the area investigated should be sufficiently known. Uplift along a steep, deep-reaching fault may result in a K-feldspar discontinuity.

(5) The influence of rock composition and fabric on the usually anisotropic heat conduction and permeability may to some extent locally modify the shape of the isothermal surface T_{diff} , especially in the case of steeply dipping s-surfaces and b-axes (WENK H. R. & WENK E., 1969).

Acknowledgement

We are indebted to Dr. Th. Schneider and the late Professor Dal Vesco for their particular support of our sampling within the St. Gotthard highway tunnel under construction. Special thanks are due to Drs. G. Frapolli and H. Wanner for their guidance and valuable help on the spot during sampling within the tunnel. We thank Professors M. Frey, Basel, and D. Stöffler, Münster, as well as PD Dr. H. Kroll, Münster, for criticism and helpful comments. The technical assistance of Ms. G. v. Cölln and Mrs. I. Schmiemann in data collecting and preparation of tables and drawings is gratefully acknowledged. Financial support by the Deutsche Forschungsgemeinschaft is greatly appreciated.

References

- AMBÜHL, E. (1929): Petrographisch-geologische Untersuchungen im zentralen Gotthardmassiv südlich Andermatt. Schweiz. Mineral. Petrogr. Mitt. 9, 265-441.
- ARNOLD, A. (1970): Die Gesteine der Region Nalps-Curnera im nordöstl. Gotthardmassiv, ihre Metamorphose und ihre Kalksilikatfels-Einschlüsse. Beitr. geol. Karte Schweiz, Neue Folge 138.
- BAILEY, S. W. (1969): Refinement of an intermediate microcline structure. Amer. Mineral. 54, 1540-1545.

- BAMBAUER, H. U. (1966): Feldspat-Familie. In W. E. Tröger: Optische Bestimmung der gesteinsbildenden Minerale, Teil 2. E. Schweizerbarth'sche Verlagsbuchhandlung, Stuttgart.
- BAMBAUER, H. U. und BERNOTAT, W. H. (1976): Untersuchungen an Feldspäten aus Graniten und Gneisen des Aar- und Gotthard-Massivs im Profil des neuen Gotthard-Strassentunnels. *Fortschr. Miner.* 54, Beih. 1,6.
- BAMBAUER, H. U., BRUNNER, G. und LAVES, F. (1962): Wasserstoff-Gehalte in Quarzen aus Zerrklüften der Schweizer Alpen und die Deutung ihrer regionalen Abhängigkeit. *Schweiz. Mineral. Petrogr. Mitt.* 42, 221-236.
- BAMBAUER, H. U. und LAVES, F. (1960): Zum Adularproblem I. Adular vom Val Casatscha; Mimetischer Lamellenbau, Variation von Optik und Gitterkonstanten und ihre genetische Deutung. *Schweiz. Mineral. Petrogr. Mitt.* 40, 177-205.
- BAMBAUER, H. U. (1978): Die Gesteine des Tavetsch. Edited by Kur- und Verkehrsverein Sedrun (Schweiz).
- BERNOTAT, W. H. (1979): Die K-Feldspat-Phasen: Interpretation von Gitterkonstanten. *Fortschr. Miner.* 57, Beih. 1, 12-14.
- BERNOTAT, W. H. (1982): The microcline/sanidine transformation isograd in metamorphic regions IV. Montagne Noire (Massif Central, France) (in preparation).
- BERNOTAT, W. H. (1982): A new measure of strain in perthites: the unit area of the face of intergrowth (601) (in preparation).
- BERNOTAT, W. H. und BAMBAUER, H. U. (1980): Die Mikroklin/Sanidin-Isograde in Aar- und Gotthardmassiv. *Eclogae Geol. Helv.* 73, 559-561.
- BERNOTAT, W. H. und BAMBAUER, H. U. (1982): The microcline/sanidine transformation isograd in metamorphic regions. II. The region of Lepontine metamorphism, Central Swiss Alps. *Schweiz. Mineral. Petrogr. Mitt.* 62, 231-244.
- BERNOTAT, W. H. und MORTEANI, G. (1982): The microcline/sanidine transformation isograd in metamorphic regions III. The Western Tauern Window and Merano-Mules-Anterselva Complex (Eastern Alps). *Amer. Mineral.* 67, 43-53.
- BERNOTAT, W. H. und NIEDERMAYR, G. (1980): Adulare ostalpinen Klüfte. *Fortschr. Miner.* 58, Beih. 1, 12-14.
- BLASI, A. (1972): «Iso-microclino» ed altre varianti strutturali del K-feldspato coesistenti in uno stesso cristallo nei graniti del Massiccio dell'Argentera. *Rend. Soc. Ital. Miner. Petr.* 23, 375-411.
- BLASCHKE, R., GENTSCH, P., GRAVER-CARSTENSEN, E., LAVES, F., WEBER, L. und T. P. WOODMANN (1974): Untersuchungen an Mondstein mit 2 Schillerflächen mittels PhEEM, REM, TEM, TEM(S) und Polarisationsmikroskop. *Beitr. elektronenmikroskop. Direktabb. Oberfl.* 7, 423-438.
- BRÜCKNER, W., DE QUERVAIN, F., STEIGER, R. und WENK, E. (1967): Exkursion Aäldorf-Gotthard-Bellinzona. *Geol. Führer Schweiz* 5, 380-399, Verlag Wepf Basel.
- BURNHAM, C. W. (1962): IBM computer program for least squares refinement of crystallographic lattice constants. *Geophys. Lab. Carnegie Inst., Washington D.C., Year Book* 61, 132-135.
- ČERNÝ, P. and MACEK, J. (1974): Petrology of potassium feldspars in two Lithium-bearing pegmatites, In: Mackenzie, W. S. and Zussman, J. (eds.): *The feldspars*. Manchester Univ. Press.
- COLLERSON, K. D. (1976): Composition and structural state of alkali feldspars from high-grade metamorphic rocks, central Australia, *Amer. Mineral.* 61, 200-211.
- DE PIERI, R. (1979): Cell dimensions, optic axial angle and structural state in triclinic K-feldspars of the Adamello massif. *Mem. Sc. Geol. Padua* 32, 1-17.
- DIETRICH, R. V. (1962): K-Feldspar structural states as petrogenetic indicators. *Norsk. Geol. Tidsskr.* 42, 394-414.
- DORA, O. Ö. (1976): Die Feldspäte als petrogenetischer Indikator im Menderes-Massiv (West-Anatolien). *Neues Jahrb. Mineral. Abhandl.* 127, 289-310.

- EULER, R. und HELLNER, E. (1961): Hydrothermale und röntgenographische Untersuchungen an gesteinsbildenden Mineralen, VI. Über hydrothermal triklinen K-Feldspat. *Z. Krist.* 115, 5/6, 28-438.
- EGGLETON, R. A. (1979): The ordering path for igneous K-felspar megacrysts. *Amer. Mineral.* 64, 906-911.
- EVANS, B. W. & TROMMSDORFF, V. (1970): Regional Metamorphism of Ultramafic Rocks in the Central Alps: Parageneses in the System CaO-MgO-SiO₂-H₂O. *Schweiz. Mineral. Petrogr. Mitt.* 50/3, 481-492.
- FREY, M. (1969): Die Metamorphose des Keupers vom Tafeljura bis zum Lukmanier-Gebiet. *Beitr. geol. Karte Schweiz, Neue Folge* 137.
- FREY, M. (1974): Alpine Metamorphism of Pelitic and Marly Rocks of the Central Alps. *Schweiz. Mineral. Petrogr. Mitt.* 54, 489-506.
- FREY, M., HUNZIKER, J. C., FRANCK, W., BOCQUET, J., DAL PIAZ, G. V., JÄGER, E. and NIGGLI, E. (1974): Alpine Metamorphism of the Alps. A Review. *Schweiz. Mineral. Petrogr. Mitt.* 54, 247-296.
- FREY, M., BUCHER, K., FRANK, E. and MULLIS, J. (1980): Alpine Metamorphism along the Geotransverse Basel-Chiasso. A Review. *Eclogae Geol. Helv.* 73, 527-546.
- GOLDSMITH, J. R. and LAVES, F. (1954): The microcline-sanidine stability relations. *Geochim. Cosmochim. Acta* 5, 1-19.
- GOLDSMITH, J. R. and LAVES, F. (1961): Polymorphism, order, disorder, diffusion and confusion in the feldspars. *Cursillos y Conferencias VIII*, 71-80.
- GUIDOTTI, C. V., HERD, H. H. and TUTTLE, C. L. (1973): Composition and structural state of K-feldspars from K-feldspar and sillimanite grade rocks in north-western Maine. *Amer. Mineral.* 58, 705-716.
- GYSIN, M. (1948): Les feldspaths potassiques des granites de Gastern et de quelques granites de l'Aar. *Schweiz. Mineral. Petrogr. Mitt.* 28, 230-245.
- HAFNER, ST. (1958): Petrographie des Südwestlichen Gotthardmassivs. *Schweiz. Mineral. Petrogr. Mitt.* 38, 255-362.
- HAFNER, ST. HARTMANN, P. und LAVES, F. (1962): Magnetische Resonanz von Al²⁷ in Adular. Zur Deutung der Adularstruktur. *Schweiz. Mineral. Petrogr. Mitt.* 42, 277-294.
- HAFNER, ST. und LAVES, F. (1957): Ordnung/Unordnung und Ultrarotabsorption II. Variation der Lage und Intensität einiger Absorptionen von Feldspäten. Zur Struktur von Orthoklas und Adular. *Z. Krist.* 109, 204-225.
- HAFNER, ST. und LAVES, F. (1963): Magnetische Kernresonanz von Al²⁷ an einigen Orthoklasen. *Schweiz. Mineral. Petrogr. Mitt.* 43/1, 65-69.
- HAFNER, ST. und LOIDA, A. (1980): Origin and variation of the microcline triclinicity in granitic bodies of the Central Alps. *Eclogae Geol. Helv.* 73, 563-570.
- HISS, B. (1978): Feldspäte als petrogenetische Indikatoren in granitoiden Gneisen des Lepontins. *Schweiz. Mineral. Petrogr. Mitt.* 58, 243-288.
- HOFMÄNNER, F. J. (1964): Petrographische Untersuchung der granitoiden Gesteine zwischen Gotthard- und Witenwasserrenreuss. *Dissertation Univ. Zürich.*
- HOVIS, G. L. (1974): A solution calorimetric and x-ray investigation of the Al-Si distribution in monoclinic potassium feldspars. In: Mackenzie, W.S. and Zussman, H. (eds.): *The feldspars.* Manchester Univ. Press.
- HUBER, H. M. (1943): Physiographie und Genesis der Gesteine im südöstlichen Gotthardmassiv. *Schweiz. Mineral. Petrogr. Mitt.* 23, 72-260.
- HUBER, W. (1948): Petrographisch-mineralogische Untersuchungen im südlichen Aarmassiv. *Schweiz. Mineral. Petrogr. Mitt.* 28/2, 555-642.
- HÜGL, TH. (1941): Zur Petrographie des östlichen Aarmassivs und des Kristallins von Tamins. *Schweiz. Mineral. Petrogr. Mitt.* 21, 1-119.

- HÜGI, TH. (1956): Vergleichende petrologische und geochemische Untersuchungen an Graniten des Aarmassivs. Beitr. Geol. Karte Schweiz. N. F. 94.
- JÄGER, E. (1973): Die alpine Orogenese im Lichte der radiometrischen Altersbestimmung. *Eclogae Geol. Helv.* 66, 11–21.
- JÄGER, E.; NIGGLI, E. und WENK, E. (1967): Rb-Sr-Altersbestimmungen an Glimmern der Zentralalpen, Beitr. Geol. Karte der Schweiz, N. F. 134.
- KARL, F. (1959): Vergleichende petrographische Studien an den Tonalitgraniten einiger periadriatischer Intrusiv-Massive. *Jahrb. Geol. Bundesanstalt Wien*, 102, 1–192.
- KROLL, H. (1968): Programm JAGOKOR zur Dehnungs- und Schrumpfungskorrektur von Röntgenfilmen (Pulverdiagrammen). Inst. Min. Univ. Münster.
- KROLL, H. (1971): Feldspäte im System $K[AlSi_3O_8]-Na[AlSi_3O_8]-Ca[Al_2Si_2O_8]$: Al,Si-Verteilung und Gitterparameter, Phasen-Transformationen und Chemismus. Inaug.-Diss., Westf. Wilhelms-Univ. Münster.
- KROLL, H. (1973): Estimation of the Al,Si-distribution of Feldspars from the Lattice Translations $Tr[110]$ and $Tr[1\bar{1}0]$. I. Alkali Feldspars. *Contr. Mineral. Petrol.* 39, 141–156.
- KROLL, H. (1980a): Estimation of the Al,Si-distribution of alkali feldspars from lattice translations $tr[110]$ and $tr[1\bar{1}0]$. Revised diagrams. *N. Jahrbuch Miner. Mh.* 1, 31–36.
- KROLL, H. (1980b): Struktur und Metrik der Feldspäte. Habilitationsschrift, Fachbereich Chemie, Univ. Münster.
- LABHART, T. P. (1977): Aarmassiv und Gotthardmassiv. *Sammlung Geol. Führer* 63, Gebr. Bornträger, Berlin.
- LAVES, F. (1950): The lattice and twinning of microcline and other potash feldspars. *J. Geol.* 58, 548–571.
- LAVES, F. (1952): Phase relations of the alkali feldspars. Part II. *J. Geol.* 60, 549–574.
- LAVES, F. (1960): Al/Si-Verteilung, Phasen-Transformationen und Namen der Alkalifeldspäte. *Z. Krist.* 113, 265–296.
- LAVES, F. and GOLDSMITH, J. R. (1961): Polymorphism, order, disorder, diffusion and confusion in the feldspars. *Cursillos y Conferencia VIII*, 71–80.
- LAVES, F. und SOLDATOS, K. (1963): Die Albit/Mikroclin-Orientierungs-Beziehungen in Mikroclin-perthiten und deren genetische Deutung. *Z. Krist.* 118, 69–102.
- LAVES, F. and VISWANATHAN, K. (1967): Relations between optic axial angle and triclinicity of potash feldspars and their significance for the definition of “stable” and “unstable” states of alkali feldspars. *Schweiz. Mineral. Petrogr. Mitt.* 47, 147–162.
- MACKENZIE, W. S. and SMITH, J. V. (1961): Experimental and geological evidence for the stability of alkali feldspars. *Cursillos y Conferencias VIII*, 53–69.
- MARFUNIN, A. S. (1961): The relation between structure and optical orientation in potash-soda feldspars. *Cursillos y Conferencias VIII*, 97–109.
- MARFUNIN, A. S. (1962): The feldspars: phase relations, optical properties and geological distribution. (Transl. from the Russian edition) Jerusalem (Israel Progr. Sci. Transl.) 317 pp.
- MCCONNELL, J. D. C. (1971): Electron optical study of phase transformations. *Min. Mag.* 38, 1–20.
- MEGAW, H. D. (1956): Notation for feldspar structures. *Acta Cryst.* 9, 56–60.
- MEGAW, H. D. (1974): The architecture of feldspars. In: Mackenzie, W. S. and Zussmann, J. (eds.): *The feldspars*; Manchester Univ. Press.
- MERGOIL-DANIEL, J. (1970): Les feldspaths potassiques dans les roches métamorphiques du Massif Central, France. *Ann. Fac. Sci. Univ. Clermont. Ser. Geol. Min.* 42.
- NEIVA, A. M. R. (1972): Sobre a microclina de alguns aplitos e pegmatitos de Alijo-Sanfins (Vila-Real), Norte de Portugal. *Memorias e Noticias, Coimbra*, 74, 5–10.
- NEIVA, A. M. R. (1974): Optic axial angle and obliquity of potassium feldspars of granites, aplites and pegmatites. In: Mackenzie, W. S. and Zussmann, J. (eds.): *The feldspars*; Manchester Univ. Press.

- NIGGLI, E. (1944): Das Westliche Tavetscher Zwischenmassiv und der angrenzende Nordrand des Gotthardmassivs. *Petrographisch-Geologische Untersuchungen. Schweiz. Mineral. Petrogr. Mitt.* 24, 58–301.
- NIGGLI, E. (1970): Alpine Metamorphose und alpine Gebirgsbildung. *Fortschr. Miner.* 47, 16–26.
- NIGGLI, E. (1974): Alpine Metamorphose von Erzvorkommen der Schweizer Alpen. *Schweiz. Mineral. Petrogr. Mitt.* 54, 595–608.
- NISSEN, H. U. (1967): Domänengefüge, Natriumgehalt, Natriumentmischung und Gitterkonstanten von Alkalifeldspäten (Mikroklin, Orthoklas, Adular) der Schweizer Alpen. *Schweiz. Mineral. Petrogr. Mitt.* 47, 1140–1145.
- POTY, B. P. STALDER, H. A. and WEISBROD, A. M. (1974): Fluid Inclusion Studies in Quartz from Fissures of Western and Central Alps. *Schweiz. Mineral. Petrogr. Mitt.* 54, 717–752.
- RAASE, P. and MORTEANI, G. (1976): The potassic feldspar in metamorphic rocks from the western Hohe Tauern area, eastern Alps. *Geol. Rundschau* 65, 422–436.
- RAITH, M. (1971): Seriengliederung und Metamorphose im östlichen Zillertaler Hauptkamm (Tirol, Österreich). *Verh. Geol. Bundes-Anstalt Wien* 1, 163–207.
- V. RAUMER, J.-F. (1967): Kristallisation und Gefügebildung im Mont-Blanc-Granit. *Schweiz. Mineral. Petrogr. Mitt.* 47, 499–579.
- RIBBE, P. H. (1975): The Chemistry, Structure and Nomenclature of Feldspars. *Min. Soc. Amer. Short Course notes, Vol. 2, Feldspar Mineralogy*, R1–R52.
- RIBBE, P. H. and GIBBS, G. V. (1975): The crystal structure of a strained intermediate microcline in cryptoperthitic association with a low albite. *Geol. Soc. Amer., Abstracts Progr. vol. 7, No. 7*, p. 1245.
- RIEDERER, J. (1965): Die Kalifeldspäte der moldanubischen Granite. *N. Jahrb. Miner. Abh.* 102, 291–339.
- RYBACH, L. (1976): Die Schweizer Geotraverse Basel–Chiasso. Eine Einführung. *Schweiz. Mineral. Petrogr. Mitt.* 56, 581–588.
- RYBACH, L., MUELLER, ST., MILNES, A. G., ANSORGE, J., BERNOULLI and FREY, M. (1980): The Swiss Geotraverse Basel–Chiasso – a review. *Eclogae Geol. Helv.* 73, 437–462.
- SCHINDLER, C. (1972): Zur Geologie der Gotthard-Nordrampe der Nationalstrasse N2. *Eclogae Geol. Helv.* 65, 301–423.
- SEEMANN, U. (1975): Mineralogisch-petrographische und geochemische Untersuchungen der granitischen Gesteine der Val Punteglias (GR). *Schweiz. Mineral. Petrogr. Mitt.* 55, 257–306.
- SIPLE, P. J. and YUND, R. A. (1974): Kinetics of Al/Si disordering in alkali feldspars. A. W. Hoffmann, B. J. Giletti, M. S. Yoder and R. A. Yund (eds.): *Geochemical Transports and Kinetics*, p. 185–193, Academic Press New York.
- SMITH, J. V. (1974): *Feldspar Minerals*, vol. 1, Springer Verlag Berlin.
- STECK, A. und BURRI, G. (1971): Chemismus und Paragenese von Granaten aus Granitgneisen der Grünschiefer- und Amphibolitfazies der Zentralalpen. *Schweiz. Mineral. Petrogr. Mitt.* 51, 534–538.
- STECK, A. (1976): Albit-Oligoklas-Mineralgesellschaften der Persteritlücke aus alpinmetamorphen Granitgneisen des Gotthardmassivs. *Schweiz. Mineral. Petrogr. Mitt.* 56, 269–292.
- STEIGER, R. H. (1962): Petrographie und Geologie des südlichen Gotthard-Massivs zwischen St. Gotthard und Lukmanierpass. *Schweiz. Mineral. Petrogr. Mitt.* 42, 381–577.
- STEIGER, R. H. und HART, S. R. (1967): The Microcline-Orthoclase Transition within a Contact Aureole. *Amer. Mineral.* 52, 87–116.
- STEWART, D. B. (1975): Optical properties of alkali feldspars. *Mineral. Soc. Amer. Short Course Notes, vol. 2, Feldspar Mineralogy*, St 23–St 30.
- STEWART, D. B. and RIBBE, P. H. (1969): Structural explanation for variation in cell parameters of alkali feldspar with Al/Si ordering. *Amer. J. Sci.* 267-A, 444–462.
- STEWART, D. B. and WRIGHT, T. L. (1974): Al,Si order and symmetry of natural alkali feldspars, and

- the relationship of strained cell parameters to bulk composition. *Bull. Soc. Franc. Mineral. Cristallogr.* 97, 350-377.
- STROB, W. D. (1982): *Metrische Variation in einer Tief-Albit/Tief-Mikroclin-Reihe und Strukturverfeinerung eines Tief-Mikroklins von Prilep (Jugoslawien)*. Dissertation Univ. Münster (in Vorbereitung).
- TOMISAKA, T. (1962): On order-disorder transformation and stability range of microcline under high vapor pressure. *Mineral J. (Tokyo)* 3, 261-281.
- VISWANATHAN, K. (1968): *Properties of Quartzes and Feldspars from Pegmatites (Ticino, Switzerland)*. Thesis, Swiss Fed. Inst. Technology, Zürich.
- VOLL, G. (1969): *Klastische Mineralien aus den Sedimentserien der Schottischen Highlands und ihr Schicksal bei aufsteigender Regional- und Kontaktmetamorphose*. Habilitationsschrift Techn. Univ. Berlin.
- VOLL, G. (1976): *Recrystallization of Quartz, Biotite and Feldspars from Erstfeld to the Leventina Nappe, Swiss Alps, and its Geological Significance*. *Schweiz. Mineral. Petrogr. Mitt.* 56, 641-647.
- WAGNER, G. A., REIMER, G. M. and JÄGER, E. (1977): *Cooling Ages derived by Apatite Fissiontrack, Mica Rb-Sr and K-Ar Dating: The Uplift and Cooling History of the Central Alps*. *Mem. Ist. Geol. Min. Univ. Padua* 30, 1-27.
- WEIBEL, M. (1961): *CHEMISCHE UNTERSUCHUNGEN AN ALPINEN KLUFTMINERALIEN*. *SCHWEIZ. MINERAL. PETROGR. MITT.* 41, 8-11.
- WENK, H. R. (1967): *Triklinität der Alkalifeldspäte in leontinischen Gneisen*. *Schweiz. Mineral. Petrogr. Mitt.* 47, 129-146.
- WENK, E. (1962): *Plagioklas als Indexmineral in den Zentralalpen. Die Paragenese Calcit-Plagioklas*. *Schweiz. Mineral. Petrogr. Mitt.* 42, 139-152.
- WENK, E. und KELLER, F. (1969): *Isograde in Amphibolitserien der Zentralalpen*. *Schweiz. Mineral. Petrogr. Mitt.* 49, 157-198.
- WERNER, D. (1980): *Probleme der Geothermik im Bereich der Schweizer Zentralalpen*. *Eclogae Geol. Helv.* 73, 513-525.
- WERNER, D., KÖPPEL, V., HÄNNY, R. and RYBACH, L. (1976): *Cooling Models for the Lepontine Area (Central Swiss Alps)*. - *Schweiz. Mineral. Petrogr. Mitt.* 56/3, 661-667.
- WINTERHALTER, R. U. (1930): *Zur Petrographie und Geologie des östlichen Gotthardmassivs*. *Schweiz. Mineral. Petrogr. Mitt.* 10, 38-116.
- WRIGHT, T. L. (1967): *The Microcline-Orthoclase Transformation in the Contact Aureole of the Eldora Stock, Colorado*. *Amer. Mineral.* 52, 117-136.
- WRIGHT, T. L. (1968): *X-ray and optical study of alkali feldspar II. An x-ray method for determining the composition and structural state from measurement of 2 θ values for three reflections*. *Amer. Mineral.* 53, 88-104.
- WRIGHT, T. L. and STEWART, D. B. (1968): *X-ray and optical study of alkali feldspar I. Determination of composition and structural state from refined unit cell parameters and 2V*. *Amer. Mineral.* 53, 38-87.
- WINCHELL, A. N. and WINCHELL, H. (1951): *Elements of optical Mineralogy. II. Description of Minerals*. Chapman and Hall Ltd., London.
- WÜTHRICH, H. (1965): *Rb-Sr-Altersbestimmungen am alpin-metamorph-überprägten Aar-Massiv*. *Schweiz. Mineral. Petrogr. Mitt.* 45, 875-971.
- YUND, R. A. and ANDERSON, T. F. (1974): *Oxygen Isotope exchange between potassium feldspar and KCl solution*. In: A. W. Hoffmann, B. J. Giletti, H. S. Yoder and R. A. Yund (eds.): *Geochemical Transports and Kinetics*, p. 185-193; Academic Press, New York.